

Dormant Comets Among the Near-Earth Object Population: A Meteor-Based Survey

Quan-Zhi Ye (叶泉志)

Department of Physics and Astronomy, The University of Western Ontario, London,
Ontario N6A 3K7, Canada

qye22@uwo.ca

and

Peter G. Brown, Petr Pokorný

Department of Physics and Astronomy, The University of Western Ontario, London,
Ontario N6A 3K7, Canada

Received _____; accepted _____

ABSTRACT

Dormant comets in the near-Earth object (NEO) population are thought to be involved in the terrestrial accretion of water and organic materials. Identification of dormant comets is difficult as they are observationally indistinguishable from their asteroidal counterparts, however they may have produced dust during their final active stages which potentially are detectable today as weak meteor showers at the Earth. Here we present the result of a reconnaissance survey looking for dormant comets using 13 567 542 meteor orbits measured by the Canadian Meteor Orbit Radar (CMOR). We simulate the dynamical evolution of the hypothetical meteoroid streams originated from 407 near-Earth asteroids in cometary orbits (NEACOs) that resemble orbital characteristics of Jupiter-family comets (JFCs). Out of the 44 hypothetical showers that are predicted to be detectable by CMOR, we identify 5 positive detections that are statistically unlikely to be chance associations, including 3 previously known associations. This translates to a lower limit to the dormant comet fraction of $2.0 \pm 1.7\%$ in the NEO population and a dormancy rate of $\sim 10^{-5} \text{ yr}^{-1}$ per comet. The low dormancy rate confirms disruption and dynamical removal as the dominant end state for near-Earth JFCs. We also predict the existence of a significant number of meteoroid streams whose parents have already been disrupted or dynamically removed.

Subject headings: comets: general, minor planets, asteroids: general, meteorites, meteors, meteoroids.

1. Introduction

Dormant comets are comets that have depleted their volatiles and are no longer ejecting dust¹. Due to their inactive nature, dormant comets cannot be easily distinguished from their asteroidal counterparts by current observing techniques (e.g. Luu & Jewitt 1990). As the physical lifetime of a comet is typically shorter than its dynamical lifetime, it is logical that a large number of defunct or dormant comets exist (Wiegert & Tremaine 1999; Di Sisto et al. 2009). Dormant comets in the near-Earth object (NEO) population are of particular interest, as they can impact the Earth and contribute to the terrestrial accretion of water and organic materials as normal comets (e.g. Hartogh et al. 2011, and the references therein).

It has long been known that the dust produced by Earth-approaching comets can be detected as meteor showers at the Earth (e.g. Schiaparelli 1866, 1867). Dormant comets, though no longer being currently active, may have produced dust during their final active phases, which are potentially still detectable as weak meteor showers. This has a significant implications for the investigation of dormant comets, as any cometary features of these objects are otherwise no longer telescopically observable. Past asteroid-stream searches have revealed some possible linkages, the most notable being (3200) Phaethon and the Geminids (e.g. Williams & Wu 1993; de León et al. 2010; Jewitt et al. 2013, and many others) as well

¹We note that the term “extinct comet” is also frequently used in the literature. Strictly speaking, “dormant comet” is usually associated with comets that only temporarily lose the ability to actively sublimate, while the term “extinct comet” usually refers to the cometary nuclei that have permanently lost the ability to sublimate (c.f. Weissman et al. 2002, for a more comprehensive discussion). However, in practice, it is difficult to judge whether the comet is temporarily or permanently inactive. In this work we use the general term “dormant comet” which can mean either scenario.

as (196256) 2003 EH₁ and the Quadrantids (Jenniskens 2004; Abedin et al. 2015), both involving meteor showers that are exceptional in terms of activity. However, most showers are weak in activity, making parent identification difficult.

Radar was introduced into meteor astronomy in the 1940s and has developed into a powerful meteor observing technique (c.f. Ceplecha et al. 1998). Radar detects meteors through the reflection of transmitted radio pulses from the ionized meteor trail formed during meteor ablation. Radar observations are not limited by weather and/or sunlit conditions and are able to detect very faint meteors. The Canadian Meteor Orbit Radar (CMOR), for example, has recorded about 14 million meteor orbits as of May 2016, which is currently the largest dataset for meteor orbits and hence a powerful tool to investigate weak meteor showers.

Efforts have been made to the search for dormant comets for several decades. Among the early attempts, Kresak (1979) discussed the use of the Tisserand parameter (Tisserand 1891) as a simple dynamical indicator for the identification of dormant comets. Assuming Jupiter as the perturbing planet, the Tisserand parameter is defined as

$$T_J = \frac{a_J}{a} + 2\sqrt{\frac{a(1-e^2)}{a_J}} \cos i \quad (1)$$

where a_J is the semi-major axis of Jupiter, and a , e , and i are the semi-major axis, eccentricity, and inclination of orbital plane of the small body. A small body is considered dynamically comet-like if $T_J \lesssim 3$. An asteroid with $T_J \lesssim 3$ is classified as an asteroid in cometary orbit (ACO). Note that dormant comets and ACOs are not all physically comets originate from the Kuiper belt, as a fraction of ACOs might originate from the main asteroid belt (e.g. Binzel et al. 2004). Separation of main belt interlopers is difficult, but attempts have been made both dynamically (e.g. Fernández et al. 2002; Tancredi 2014) and spectroscopically to separate possible cometary nuclei from asteroidal bodies

(e.g. Fernández et al. 2005; DeMeo & Binzel 2008; Licandro et al. 2016). However, few attempts have been made to link ACOs with meteor showers. Jenniskens (2008) provided a comprehensive review of meteoroid streams possibility associated with dormant comets based on the similarity between their orbits, but a comprehensive contemporary “cued” survey to look for all possible weak streams from the large number of recently discovered ACOs/NEOs that may have had weak past activity, including formation of early meteoroid trails, is yet to be performed.

In this work, we present a survey for dormant comets in the ACO component in the NEO population through the meteoroid streams they might have produced during their active phase, using the most complete CMOR dataset available to date. The survey is performed in a “cued search” manner rather than a commonly-used blind search: we first identify eligible ACOs (i.e. with well-determined orbits suitable for long-term integration) in the NEO population (§ 2), then simulate the formation and evolution of the meteoroid trails produced by such ACOs assuming they have recently been active (§ 3), and then search the CMOR data using the virtual shower characteristics to identify “real” streams now visible at the Earth (§ 4). Our survey thus simulates *all* near-Earth ACOs (NEACOs) which are now known and which would have produced meteor showers at the Earth if they were recently active. This approach accounts for orbital evolution of the parent *and* the subsequent evolution of the virtual meteoroid stream.

2. Identification of Potential Shower-Producing Objects

2.1. Dormant Comets in the NEO Population

To establish the starting conditions for the survey, we first identify possible dormant comets in the NEO population. By definition, NEOs have perihelion distance $q < 1.3$ AU.

In this work we focus our sampling among the orbit range of Jupiter-family comets or JFCs which overlaps the NEO population (near-Earth JFCs or NEJFCs as used by other authors). We use a slightly more relaxed constraint than the original Tisserand’s derivation, namely $1.95 < T_J < 3.05$. This is because the Tisserand parameter is derived assuming restricted three-body problem with a circular orbit of the planet; in reality, T_J is only an approximate, since the orbit of the planet is never strictly circular, as well as the fact that the small body is also perturbed by other planets (e.g. Murray & Dermott 1999, p.73). We also consider the precision of the perturbed orbit solution, which is parameterized as the Uncertainty Parameter, U (see Marsden et al. 1978). We only consider objects with $U \leq 2$, as objects falling into this category are considered “secure” and will be permanently numbered². With these criteria, we identify a total of 407 objects from 13 763 known NEOs as of 2016 February 9. These 407 ACOs in the NEO population represent possible dormant comets which may have produced meteoroid streams in the recent past.

2.2. Objects with Detectable Meteor Showers

The next step is to simulate the “virtual” meteoroid stream of each object to see if a meteor shower is currently detectable by CMOR. Following the discussion in Ye et al. (2016a), the meteoroid flux \mathcal{F} at Earth can be calculated by

$$\mathcal{F} = \frac{\eta N_{\text{in}} \tau_{\text{stream}}}{P^2 \Delta t_{\text{shower}}^2 V_{\oplus}^2} \quad (2)$$

where η is the fraction of *potentially visible meteoroids*, a subset of the Earth-bound meteoroids that may be visible as meteors, defined as meteoroids with Minimum Orbital

²See <http://www.minorplanetcenter.org/iau/info/UValue.html>, retrieved 2016 February 10.

Intersection Distance (MOID) < 0.01 AU with respect to the Earth’s orbit (typical cross-section of meteoroid stream, see Brown & Jones 1998; Göckel & Jehn 2000); N_m is the meteoroid/dust production of the parent, which we take $N_m \sim 10^{15}$ per orbit as a median case for near-Earth JFCs (elaborated in Appendix A); τ_{stream} is the age of the meteoroid stream; P is orbital period of the parent; Δt_{shower} is the duration of the meteor shower (defined by half-width-half-maximum of the shower), and $V_{\oplus} = 30 \text{ kms}^{-1}$ is the orbital speed of the Earth.

The CMOR-observed flux will be different from \mathcal{F} as the detection efficiency of CMOR is a function of the meteoroid arrival speed (Figure 1) and meteoroid stream size distribution (Figure 2). For each virtual stream, we assign η_{CMOR} being the CMOR detection efficiency, as

$$\mathcal{F}_{\text{CMOR}} = \eta_{\text{CMOR}} \cdot \mathcal{F} \quad (3)$$

There remain four unknown variables: η , τ_{stream} , Δt_{shower} and η_{CMOR} . Typical numbers for the first three variables are $\eta \sim 0.1$ (i.e. 1 out of every 10 simulated meteoroids will reach the Earth), $\tau_{\text{stream}} \sim \text{a few } 10^2 \text{ yr}$ and $\Delta t_{\text{shower}} \sim \text{a few days}$, but all of these quantities are highly variable (McIntosh & Hajduk 1983; Cremonese et al. 1997; Jenniskens 2006). For our survey we compute all of these quantities per object (and the fourth variable, η_{CMOR}) numerically using the following procedure.

We define τ_{stream} first as the other three variables depend on it. Simulations are performed using the MERCURY6-based (c.f. Chambers 1999) meteoroid model developed in our earlier works (e.g. Ye & Hui 2014; Ye et al. 2015). We employ the ejection model described by Jones (1995) for meteoroids with sizes between 0.5 and 50 mm, an “envelop” size range appropriate to the detection range of CMOR as given by the meteoroid ablation model (Figure 1, c.f. Campbell-Brown & Koschny 2004), assuming a bulk density of

$1\,000\text{ kg} \cdot \text{m}^{-3}$ and a size distribution of $dN/da \propto a^{-q}$ where $q = 3.6$ (Fulle 2004, § 5). Meteoroids are released in a time step of 10 d when the parent is within the sublimation line ($r_h < 2.3\text{ AU}$). The system of planets, parent bodies and meteoroids are then integrated with the RADAU integrator (Everhart 1985) with an initial time step of 7 d. Time step is reduced upon close encounters as documented in Chambers & Migliorini (1997). Gravitational perturbations from the eight major planets (with the Earth-Moon system represented by a single mass at the barycenter of the two bodies), radiation pressure, and Poynting-Robertson effect are considered in the integration.

We operationally define τ_{stream} as the time taken for the median D -parameter of any two test meteoroids to grow beyond a given threshold. The D -parameter was originally introduced by Southworth & Hawkins (1963) for meteor shower identification; it is essentially a measure of the similarity between a pair of orbits denoted as A and B :

$$D_{A,B}^2 = (q_B - q_A)^2 + (e_B - e_A)^2 + \left(2 \sin \frac{I}{2}\right)^2 + \left[(e_A + e_B) \sin \frac{\Pi}{2}\right]^2 \quad (4)$$

where

$$I = \arccos [\cos i_A \cos i_B + \sin i_A \sin i_B \cos (\Omega_A - \Omega_B)] \quad (5)$$

$$\Pi = \omega_A - \omega_B + 2 \arcsin \left(\cos \frac{i_A + i_B}{2} \sin \frac{\Omega_A - \Omega_B}{2} \sec \frac{I}{2} \right) \quad (6)$$

and the subscripts A and B refer to the two orbits being compared. Here q is the perihelion distance in AU, e is the eccentricity, i is the inclination, Ω is the longitude of ascending node, and ω is the argument of perihelion. The sign of the arcsin term in the equation for Π switches if $|\Omega_A - \Omega_B| > 180^\circ$.

The physical meaning of τ_{stream} can be interpreted as a measure of the dispersion timescale of the meteoroid stream, equivalent to the age of the stream.

For each object, the simulation starts with $\tau_{\text{stream}} = 100$ yr. This value is incremented in steps of 100 yr, until the median D -parameter among all test particles that composed the virtual stream reaches $D = 0.1$, an empirical cutoff that was found by Southworth & Hawkins (1963) and was later revisited by many (e.g. Sekanina 1976; Drummond 1981; Ceplecha et al. 1998); or $\tau_{\text{stream}} = 10^4$ yr which we adopt as an operational upper limit for the simulation, as this is comparable to the oldest estimated stream ages based on de-coherence timescales (Pauls & Gladman 2005).

Once τ_{stream} is determined, we calculate the MOID of each test meteoroids with respect to the Earth’s orbit at the epoch of 2012 Jan. 1 Terrestrial Time and collect those with $\text{MOID} < 0.01$ AU (i.e. potentially visible meteoroids). The values of η , η_{CMOR} (the number of meteoroids detectable by CMOR size bins divided by the total number of potentially visible meteoroids) and Δt_{shower} (defined as the standard deviation of the solar longitudes of the MOID points) are readily available at this stage. The number of test meteoroids making the CMOR-detectable virtual meteor shower (not the total simulated test meteoroids which is $\sim 10^5$) at this stage is typically $\sim 10^3$ and is at least 100. The virtual meteoroid shower flux for each parent is then calculated using Eq. 2 and 3. The detection limit for multi-year CMOR data is of the order of $10^{-3} \text{ km}^{-2} \text{ hr}^{-1}$ (Bruzzone et al. 2015). Hence, we only consider virtual showers with $\mathcal{F}_{\text{CMOR}} \gtrsim 10^{-3} \text{ km}^{-2} \text{ hr}^{-1}$ as CMOR-detectable showers.

Readers may immediately notice that, for a significant fraction of the objects, the calculated τ_{stream} is beyond the typical chaotic timescale of JFCs (~ 1000 yrs, e.g. Tancredi 1995). Here it is important to note that our approach focuses at the *mean orbit* rather than the exact position of the parent; therefore we are to examine the chaotic timescale of the orbit instead of the parent. For each object, we generate 100 clones from the covariance

matrix of the orbital elements³ and integrate them backward in time. Similar to the definition of τ_{stream} , we define the parental orbital chaotic timescale τ_{parent} as the time taken for the median D -parameter of any two clones to grow beyond 0.1. Thus, τ_{parent} corresponds to the time that the parent orbit is well constrained and the associated meteoroid stream can therefore be simulated with confidence. The value of τ_{stream} should be viewed cautiously if $\tau_{\text{parent}} \ll \tau_{\text{stream}}$.

Following this procedure, we identify 44 objects that meet both our visibility and detection criteria, and that the stream formation process have the potential of producing CMOR-detectable meteor activity between 2002 and 2015. Note that no geographic constraint is considered at this stage; i.e. southerly virtual radiants are still included. Detailed results are tabulated in Table 1 and in Appendix B. The values of τ_{parent} and τ_{stream} for each object are also listed. Several known asteroid-stream linkages are among the list, such as (196256) 2003 EH₁ – Quadrantids (Jenniskens 2004; Abedin et al. 2015) and 2004 TG₁₀ – Taurid complex (Jenniskens 2006; Porubčan et al. 2006). For these established linkages, the calculated radiants and arrival speeds agree with observations within uncertainties, providing some basic validation of the meteoroid modeling approach. In particular, we note that the calculated stream ages (τ_{stream}) are 300 yr for Quadrantids and 6100 yr for the 2004 TG₁₀ component in the Taurid complex, consistent with previous findings (200 yr for Quadrantids and $\sim 10^4$ yr for Taurids, e.g. Steel et al. 1991; Abedin et al. 2015). Additionally, our model predicts a flux of $0.012 \text{ km}^{-2} \text{ hr}^{-1}$ for the Quadrantids to CMOR’s limiting sensitivity, broadly consistent with daily average fluxes of a few $0.01 \text{ km}^{-2} \text{ hr}^{-1}$ (e.g. Brown et al. 1998). The modeled flux for the Taurids, however, is about 100 times higher than observations, likely related to the formation mechanism of the Taurids not being purely sublimation-driven (c.f. Jenniskens 2006, § 25, and the

³Available from the JPL Small-Body Database, retrieved on 2016 February 15.

references therein) which differs from our modeling assumption.

3. Prediction of Virtual Meteor Showers

Meteor activity is classified into two categories: annual showers, which are visible every year at more or less the same time and rate; and outbursts, which are enhancements visible in some years but not others. This divide plainly reflects the evolution of the meteoroid cloud: recently-formed meteoroid *trails* experience little differential effects due to radiation pressure and planetary perturbation, and thus tend to remain concentrated in a narrow arc in the orbit and only become visible as meteor outbursts when this “knot” of denser material impacts the Earth. After some time, differential effects gradually stretch the trail along the entire orbit into a meteoroid *stream*, visible as an annual meteor shower every time the Earth arrives at the stream intersection point. Outbursts from young trails provide clues to the ejection state (epoch, particle ejection speed, etc.) of the trails, such as the case of 55P/Tempel-Tuttle and the Leonids (e.g. Yeomans et al. 1996). In contrast, more highly evolved streams are useful for the estimation of the age of the entire stream, such as the case of 109P/Swift-Tuttle and the Perseids (e.g. Brown & Jones 1998).

For the prediction of annual showers, we use the simulation result obtained in § 2.2 and calculate the radiant and timing of the potentially visible meteoroids at the Earth. Results are tabulated in Table 1. The values of τ_{parent} and τ_{stream} are also listed in the same table. We find the median τ_{parent} to be 4300 yr, comparable to the typical timescale of 100% growth in the positional uncertainty of a JFC (Tancredi 1995). For individual bodies, τ_{parent} depends on the dynamical characteristics of the body as well as the precision of the observation. Objects with extremely long τ_{parent} are usually found in/near mean-motion resonances, and/or observed by high-precision techniques (e.g. radar observations). The median τ_{stream} is found to be ~ 1800 yr, which is also consistent with other studies (e.g.

Babadzhanov & Obruchov 1992; Jenniskens 2006, §26.1).

For the prediction of meteor outbursts, we first probe the transition timescale from trail to stream, or simply the *encircling time* of the meteoroid cloud, τ_{enc} . In another sense, τ_{enc} corresponds to the time that the ejection state of a meteoroid trail is preserved. We define τ_{enc} as the time taken for the standard deviation of the mean anomalies of the meteoroids to reach 60° (The mathematical consideration is that 99.7% or 3σ of the meteoroids spread to half orbit or 180° in mean anomaly assuming a Gaussian distribution). The simulation is conducted in the same manner as the simulation in § 2.2. We then follow the evolution of the meteoroid trail formed by each parent up to τ_{enc} years preceding 2012 AD and search for encounters between the trails and the Earth in CMOR-operational years (2002–2015). For each encounter, we estimate the meteoroid flux following the method described in Ye et al. (2016b) taking the median JFC model for dust production of the parent. We only consider encounters with the Earth’s orbit of less than ~ 0.002 AU (c.f. the discussion regarding the “second space criterion” in Vaubaillon et al. 2005) and predicted meteoroid flux $\mathcal{F}_{\text{CMOR}} > 10^{-2} \text{ km}^{-2} \text{ hr}^{-1}$, the detection limit of single year CMOR data (Ye et al. 2016b). Our model predicts 25 outburst events from a total of 11 objects that are potentially detectable by CMOR. These are tabulated in Table 4.

4. Observational Survey of Virtual Meteor Activity

The observational data for our survey is gathered by CMOR, an interferometric backscatter radar system located near London, Canada (e.g. Jones et al. 2005; Brown et al. 2008; Weryk & Brown 2012). CMOR consists of one main site equipped with interferometer as well as five remote receivers, all of which operate at 29.85 MHz (Ye et al. 2013). Orbits of the meteoroids can be derived from the interferometry and the time delay for common radar echoes between various stations. Routine and continuous observation commenced

in early 2002. As of early 2016, CMOR has measured ~ 13 million meteor orbits with a corresponding representative meteor magnitude of $\sim +7$.

Meteor showers (outbursts) are defined as an enhancement in meteor rates from a certain celestial point (the *radiant*) at a certain speed over a short period of time. The wavelet transform method has been demonstrated as a robust method for shower identification in radar data (Galligan 2000). Here we perform the survey search using a quasi 4-dimensional Mexican hat wavelet, with the wavelet coefficient $\psi(x_0, y_0, v_{g,0})$ at celestial coordinate (x_0, y_0) and speed $(v_{g,0})$ defined as:

$$\begin{aligned} \psi(x_0, y_0, v_{g,0}) = & \frac{1}{(2\pi)^{3/2}\sigma_v^{1/2}} \int_{v_{g,\min}}^{v_{g,\max}} \int_{-\infty}^{\infty} \int_{-\infty}^{\infty} f(x, y, v_g) \\ & \times [3 - g(x, y, \sigma_{\text{rad}}) - h(v_g, \sigma_v)] \\ & \times \exp \left\{ -\frac{1}{2} [g(x, y, \sigma_{\text{rad}}) - h(v_g, \sigma_v)] \right\} dx dy dv_g \end{aligned} \quad (7)$$

and

$$g(x, y, \sigma) = \frac{(x - x_0)^2 + (y - y_0)^2}{\sigma^2} \quad (8)$$

$$h(v_g, \sigma_v) = \frac{(v_g - v_{g,0})^2}{\sigma_v^2} \quad (9)$$

where $f(x, y, v_g)$ is the distribution of radiants, σ_{rad} and σ_v are the spatial and speed probe sizes, x , y and v_g are spatial coordinates and speed in the geocentric space of observed radiants.

To enhance the signal from annual weak showers, we follow the procedure described in Bruzzone et al. (2015) and combine the entire CMOR dataset into a stacked virtual

year. The data in both calendar year and stacked virtual year are divided into 1° solar longitude bins, producing a quasi 4-dimensional data-set that is then analyzed using the wavelet technique. The wavelet transform detects only radiants within roughly one spatial/speed probe size, as these contribute significantly to the wavelet coefficient. As such, radiant distributions that match the specified spatial/speed probe sizes will show enhanced wavelet coefficient. For most showers, the simulated radiants are very compact such that the spatial/speed spreads are comparable to or smaller than the CMOR’s measurement uncertainty. For these cases we use the the empirical probe sizes of 4° and 10% adopted by Brown et al. (2008) for shower detection.

For each shower/outburst, we inspect the variation of $\psi(x_0, y_0, v_{g,0})$ as a function of time within the virtual/natural year to search for enhancements. Positive detections behave as a rise in $\psi(x_0, y_0, v_{g,0})$ that is well above the background noise (e.g. Brown et al. 2010, Fig. 1).

5. Results and Discussion

5.1. Annual Showers from Old Streams

Among the 44 virtual streams predicted to be detectable by CMOR, we identify four probable positive detections in the stacked CMOR data that can be associated with (196256) 2003 EH₁, 2004 TG₁₀, 2009 WN₂₅, and 2012 BU₆₁, as shown in Figure 3. Among these associations, two are considered established: (196256) 2003 EH₁ to the Quadrantids (e.g. Jenniskens 2004; Abedin et al. 2015) and 2004 TG₁₀ as part of the Taurid complex (e.g. Jenniskens 2006; Porubčan et al. 2006); one is recently proposed: 2009 WN₂₅ to the November i Draconids (Micheli et al. 2016). For all these three cases, the predicted shower characteristics are consistent with the observations, except for the activity duration of the

November i Draconids – 2009 WN₂₅ pair. The predicted duration is about 1 day while the observed activity lasted for ~ 20 days (Brown et al. 2010). This simply reflects that we assume the operational stream age $\tau_{\text{stream}} = 100$ yr while the actual stream might be much older (and thus more dispersed). One node of the detection associated with 2012 BU₆₁ is identified with the Daytime ξ Sagittariids (descending node), which in turn has been previously associated with 2002 AU₅ (Brown et al. 2010) though the linkage is not considered well established. The ascending nodal intersection for 2012 BU₆₁ can not be identified with any known showers, but does show detectable enhancement as shown in Figure 3.

A complicating issue in the parent-shower linkage is the likelihood of chance alignment. This is especially true as there are over 14 000 known NEOs and ~ 700 identified/proposed meteor showers as of May 2016⁴. Therefore, **it is not sufficient to propose a linkage by simply noting the similarity of the respective orbits**. Instead, following the exploration by Wiegert & Brown (2004), we evaluate the following question to establish orbital similarity significance: consider the D_{SH} parameter between the proposed parent-shower pair to be D'_0 , what is the expected number of parent bodies $\langle X \rangle$ that have orbits such that $D' < D'_0$ (where D' is the D_{SH} parameter between the “new” parent and the shower)?

This question can be answered using a NEO population model providing the orbits of the possible parent and the meteoroid stream are well known. We employ the de-biased NEO model developed by Greenstreet et al. (2012) and generate two synthetic NEO populations down to absolute magnitude $H = 18$ and $H = 22$ following $\alpha = 0.35$ for

⁴<http://www.minorplanetcenter.net/mpc/summary> and http://www.astro.amu.edu.pl/~jopek/MDC2007/Roje/roje_lista.php?corobic_roje=0&sort_roje= retrieved 2016 May 7.

$H < 18$ and $\alpha = 0.26$ for $18 < H < 22$ (where α is the size distribution index of the NEO population; see Jedicke et al. 2015). Orbits of the meteoroid streams of interest are calculated from the respective wavelet maxima as found in the CMOR data. The ascending nodal activity for 2012 BU₆₁ is heavily contaminated by sporadic activity later in the year ($\lambda_{\odot} \sim 240^{\circ}$) which prevents useful orbits to be obtained. This procedure is repeated for the proposed linkages of November i Draconids – 2009 WN₂₅ and Daytime ξ Sagittariid – 2002 AU₅ and 2012 BU₆₁. The results are summarized in Table 2.

We observe the following:

1. The statistical model supports 2009 WN₂₅ as the likely parent for the November i Draconids.
2. The case of 2012 BU₆₁ and the Daytime ξ Sagittariids is complicated. The orbits derived from this work and Brown et al. (2010) is notably different from the one initially proposed in the Harvard Radio Meteor Project (Sekanina 1976, listed as ξ Sagittariids, though the IAU catalog has identified it as the same shower) which has $D_{SH} = 0.28$, though this work and Brown et al. (2010) use virtually the same data. The Daytime ξ Sagittariids has not been reported by a third observing system. However, we note that the Daytime Scutids, another unestablished shower reported by the Harvard survey, resembles the orbit of the Daytime ξ Sagittariids observed by CMOR (see Sekanina 1973, the orbit of Daytime Scutids is appended in Table 2), with $D_{SH} = 0.15$. We suspect that two different showers have been accidentally assigned the same name. The association to 2012 BU₆₁ would be statistically significant, either using the CMOR orbit or the Harvard orbit for the Daytime Scutids.
3. The linkage between 2002 AU₅ and Daytime ξ Sagittariids or Daytime Scutids is not statistically significant.

We note that among the four parent-shower associations found by our survey, three parents, namely 2004 TG₁₀, 2009 WN₂₅ and 2012 BU₆₁, are sub-kilometer bodies. Since sub-kilometer comets are effectively eliminated by rotational disruption (Rubincam 2000; Taylor et al. 2007; Jewitt et al. 2010), we think that these four bodies are likely larger fragments from previous break-ups. In fact, 2004 TG₁₀ is generally recognized as being part of the Taurid complex (Porubčan et al. 2006), while the November i Draconid streams (which 2009 WN₂₅ is linked to) has been considered to be associated with the Quadrantid stream (Brown et al. 2010).

In addition to the positive detections, we have not reproduced a number of previously proposed associations. Our initial shortlist included most of the objects in earlier proposed associations except objects with short orbital arc (i.e. low orbit quality). The calculation of $\langle X \rangle$ is repeated for every proposed association. As shown in Table 3, only 8 out of 32 previously proposed associations have $\langle X \rangle \ll 1$:

1. Corvids – (374038) 2004 HW. Linkage first proposed by Jenniskens (2006). The Corvid meteor shower is one of the slowest known meteor showers, with $v_g = 9 \text{ km s}^{-1}$. It was only observed in 1937 (Hoffmeister 1948) until being recently recovered by Jenniskens et al. (2016) and has not been detected by many radar and photographic surveys. The Corvids are undetected by CMOR, which is unsurprising as back-scatter radars are insensitive to very slow meteors.
2. ψ Cassiopeiids – (5496) 1973 NA. Linkage first proposed by Porubcan et al. (1992). The object is not included in Table 1 due to low expected flux being below the CMOR detection limit. Our test simulation shows that only a small fraction ($< 0.1\%$) of sub-millimeter-sized meteoroids ($\sim 0.1 \text{ mm}$) released in the past 1000 yr would be arriving at the Earth’s orbit. The fact that the meteor shower is detectable by video techniques (which only detect larger, millimeter-sized meteoroids) is incompatible

with the modeling result.

3. 66 Draconids – 2001 XQ. The unconfirmed shower has only been reported by Šegon et al. (2014b) who also propose the linkage. Our survey wavelet analysis at the reported radiant of the 66 Draconids did not detect any enhancement.
4. δ Mensids – (248590) 2006 CS. Linkage first proposed by Jenniskens (2006). The unconfirmed shower is only accessible by observers in the southern hemisphere.
5. ι Cygnids – 2001 SS₂₈₇. Linkage first proposed by Andreić et al. (2013) who remains the only observer of this unconfirmed shower at the time of writing. No enhancement is seen in the CMOR wavelet analysis at the reported radiant.
6. κ Cepheids – 2009 SG₁₈. Shower discovered by Šegon et al. (2015) who also propose the linkage. The predicted radiant is consistent with the reported radiant of κ Cepheids. The meteoroid speed is favorable for radar detection ($v_g = 34 \text{ km s}^{-1}$) and a relatively strong flux is predicted ($\mathcal{F} = 0.22 \text{ km}^{-2} \text{ hr}^{-1}$), however no enhancement is seen in the wavelet analysis at either the predicted or the reported radiant.
7. Northern γ Virginids – 2002 FC. Linkage proposed by Jenniskens (2006). This unestablished shower has only been reported by Terentjeva (1989) who analyzed photographic fireball observations from 1963 to 1984. No enhancement is seen in wavelet analysis of the CMOR data at the reported radiant.
8. ζ^1 Cancrids – 2012 TO₁₃₉. Shower detection as well as potential linkage are both identified by Šegon et al. (2014a). No enhancement is seen in the CMOR wavelet analysis at the predicted radiant. Also, the model predicts a stronger descending nodal shower which is also not seen in CMOR data.

It should be emphasized that the statistical test only addresses the likelihood of finding a better parent body match for a given stream orbit; it does not take into account the

false positives in shower identification, a complicated issue heavily investigated for half a century (e.g. Southworth & Hawkins 1963; Drummond 1981; Galligan 2001; Brown et al. 2008; Moorhead 2016, and many others). There exists a danger of assigning a small body as the “parent” of some random fluctuation in the meteoroid background. This is especially true for unestablished showers, as most of them have been observed by only one observer.

5.2. Outbursts from Young Trails

Among the predictions given in Table 4, only one prediction is associated with a distinct detection: the event from (139359) 2001 ME₁ in 2006 (Figure 4, 5 and Table 5). The association is of high statistical significance, as $\langle X \rangle_{H<18} \sim 0.01$. From the wavelet profile, we estimate that the observed flux is close to the detection threshold or $\sim 10^{-2} \text{ km}^{-2} \text{ hr}^{-1}$, as the signal is not very significantly higher than the background fluctuation. The event, if indeed associated with (139359) 2001 ME₁, should have originated from a relatively recent ($< 100 \text{ yr}$) ejection event. Since the observed flux is about the same order as the model prediction, it can be estimated that the dust production associated to the ejection is comparable to the average dust production of known near-Earth JFCs. Curiously, the annual shower associated with (139359) 2001 ME₁, though with a moderate expected flux, is not detected. This may suggest that the ejection was a transient event rather than a prolonged one, possibly similar to the activity of 107P/(4015) Wilson-Harrington upon its discovery in 1949 (c.f. Fernández et al. 1997).

Another interesting aspect of our survey is the negative detection of several strong predicted events (with $\mathcal{F}_{\text{CMOR}} \gtrsim 1 \text{ km}^{-2} \text{ hr}^{-1}$). These can be used to place a tight constraint on the past dust production of the parent. It can be concluded that the dust production of 2001 HA₄, 2012 TO₁₃₉ and 2015 TB₁₄₅ are either at least 2 magnitudes lower than the median near-Earth JFC model or have a much steeper dust size distribution than

we assume.

5.3. Discussion

With the results discussed above, we now revisit the population statistics of the dormant comets. We first consider the number of streams detectable by CMOR, $\mathcal{N}_{\text{CMOR}}$, to be expressed as

$$\mathcal{N}_{\text{CMOR}} = \mathcal{N}_{\text{dc}} \cdot \eta_{\text{NEACO}} \cdot \eta_{\text{shr}} \cdot \eta_{\text{CMOR}} \quad (10)$$

where \mathcal{N}_{dc} is the true (de-biased) number of dormant comets in the NEACO population, η_{NEACO} is the detection efficiency of the NEACOs (i.e. the number of known NEACOs divided by the number of total NEACOs predicted by NEO population model), η_{shr} is the selection efficiency of NEACOs that produce visible meteor showers (i.e. the number of shower-producing NEACOs divided by the total number of NEACOs), and η_{CMOR} is the detection efficiency of CMOR (i.e. the number of total virtual showers observable by CMOR divided by the total number of virtual showers visible at the Earth). Rearranging the terms, we have

$$\mathcal{N}_{\text{dc}} = \mathcal{N}_{\text{CMOR}} \cdot (\eta_{\text{NEACO}} \cdot \eta_{\text{shr}} \cdot \eta_{\text{CMOR}})^{-1} \quad (11)$$

We focus on annual shower detection in the following as the statistics for outburst detection (only 1) is too low. As presented above, we have $\mathcal{N}_{\text{CMOR}} = 2$ for $H < 18$ population and $\mathcal{N}_{\text{CMOR}} = 4$ for $H < 22$ population. For the remaining three coefficients:

1. For η_{NEACO} , we obtain the true (de-biased) number of NEACOs by using Greenstreet et al. (2012)’s NEO population model and incorporate the population

statistics from Stuart (2001), Mainzer et al. (2011) and Jedicke et al. (2015). We derive $\mathcal{N}_{\text{NEACO}} = 200 \pm 30$ for $H < 18$ and 2100 ± 300 for $H < 22$. Considering that we have selected 407 NEACOs in our initial sample, of which 199 are bodies with $H < 18$, we obtain $\eta_{\text{NEACO}} = 1_{-0.13}^{+0.00}$ for $H < 18$ and $\eta_{\text{NEACO}} = 0.19_{-0.02}^{+0.03}$ for $H < 22$.

2. For η_{shr} , we have 44 hypothetical showers as listed in Table 1, among which 15 are from $H < 18$ bodies. This yields $\eta_{\text{shr}} \sim 0.1$.
3. For η_{CMOR} , we exclude the meteoroid streams whose are either too slow for reliable radar detection ($v_g < 15 \text{ km s}^{-1}$ Weryk & Brown 2013) or have radiants too far south for CMOR to detect ($\beta < -30^\circ$). This leaves 36 streams in Table 1, including 14 originating from $H < 18$ bodies. This translates to $\eta_{\text{CMOR}} \sim 0.8$.

With all these numbers, we obtain $\mathcal{N}_{\text{dc}} = 25 \pm 21$ for $H < 18$ population and $\mathcal{N}_{\text{dc}} = 263 \pm 173$ for $H < 22$ population, with uncertainties derived by error propagation. This translates to a fraction of $\sim 10\%$ of dormant comets in the NEACO population independent of size. Assuming dormant comets in asteroidal orbits (i.e. $T_J > 3$ bodies) are negligible, we further derive a dormant comet fraction of $2.0 \pm 1.7\%$ for the entire NEO population, which should be considered as a lower limit. This number is at the low end of previous estimates by Bottke et al. (2002), Fernández et al. (2005) and Mommert et al. (2015) who give ranges of 2–14%. It should be noted that all these authors also assume that dormant comets in asteroidal orbits are negligible during the derivation of the dormant comet fraction.

There are two caveats in our work that may lead to an underestimation of the dormant comet fraction. Since we used the median of the dust production of *known* JFCs to feed the meteoroid flux model, if the actual JFC dust production is in fact lower, our treatment will lead to an overestimation of the number of visible showers, which will in turn reduce

the derived dormant comet fraction. For a dormant comet fraction of $\sim 8\%$, we need to reduce η_{shr} by a factor of $8\%/2\% = 4$, equivalent to using a dust production model that is 10 times lower than the current median model. This is qualitatively consistent with the recent trend that more weakly-active comets are being discovered as more sensitive NEO surveys become operational. Another caveat is that the actual dust size distribution q may be different than what is used in the dust model. A steeper size distribution will result in a proportionally larger number of smaller meteoroids, making the stream more dispersed and hence more difficult to be detected. This hypothesis is not supported by reported cometary observations which are found to have $q \sim 3.6$ at μm -range sizes (e.g. Fulle 2004), but a discrepancy between millimeter to sub-millimeter-sized meteoroids is possible, such as the case of 21P/Giacobini-Zinner and the Draconids (Ye et al. 2014).

Another fundamental question is, are dormant comets in asteroidal orbits really negligible? There is at least one prominent counter-example: (3200) Phaethon ($T_J = 4.508$). Phaethon is associated with the Geminid meteor shower and still possesses some outgassing activity at perihelion (e.g. Jewitt & Li 2010). Nevertheless, the fact that we do not see a lot of active NEAs suggests that such objects may not be very common.

Taking the median dynamical lifetime of near-Earth JFCs to be a few 10^3 yr, the derived dormancy rate translates to a dormancy probability of $\sim 10^{-5} \text{ yr}^{-1}$ per comet independent of sizes. This is consistent with previous model predictions, and about 5–40 times lower than the disruption probability (Fernández et al. 2002; Belton 2014). This result echoes earlier suggestions that near-Earth JFCs are more likely to be disrupted rather than achieving dormancy (Belton 2014). Since the typical timescale for JFC disruption, a JFC’s dynamical lifetime in the NEO region, and dispersion lifetime for a resulting meteoroid stream are all at the same order (a few 10^3 yr), there should exist a significant number of meteoroid streams with parents that are either disrupted or have been dynamically removed

such that no parent can be found, supporting the speculation of Jenniskens & Vaubaillon (2010) that many meteoroid streams are produced from disrupted comets. Since disruption and dynamical removal are competing mechanisms to eliminate JFCs from the NEO region, it may be difficult to investigate the formation of these “orphan” streams in the absence of an observable parent.

Finally, we compare our list against the dormant comet candidates proposed in previous works. The largest list of dormant candidates to-date is published by Tancredi (2014) and includes 203 objects that resemble JFC orbits and match a set of restrictive criteria. According to our simulations, only 3 of these 203 objects have the potential of producing CMOR-detectable activity [(196256) 2003 EH₁, 1999 LT₁, and 2004 BZ₇₄; note that not all of the objects are in our initial shortlist, as Tancredi’s list has a more relaxed constraint on orbital precision], and only 1 out of the 7 objects has a detectable shower [(196256) 2003 EH₁]. Kim et al. (2014) compiled a list of 123 NEACOs and have thermal observations, 29 of which overlap with Tancredi’s list. Among these, 3 have the potential of producing CMOR-detectable activity [(307005) 2001 XP₁, 2001 HA₄, and 2010 JL₃₃] but none of them has detectable shower. DeMeo & Binzel (2008) analyzed spectra of 49 NEOs that resemble cometary orbits (excluding 6 objects that have been later identified as comets), 6 of which may produce CMOR-detectable activity [(3360) Syrinx, (16960) 1998 QS₅₂, (137427) 1999 TF₂₁₁, (139359) 2001 ME₁, (401857) 2000 PG₃, and 1999 LT₁], only one of them produces a detectable shower, (139359) 2001 ME₁, which they reported an albedo of 0.04 and classified as a P-type asteroid. Other works (see Mommert et al. 2015; Licandro et al. 2016, and the references therein) have reported smaller samples consisting of the same objects already discussed that may produce showers from our simulations. Each author has selected a somewhat different set of candidates, but there are several objects that are selected by more than one author, including (248590) 2006 CS (which is the possible parent of δ Mensid meteor shower), (394130) 2006 HY₅₁, (436329) 2010 GX₆₂, (451124) 2009 KC₃, 1999 LT₁,

2001 HA₄ and 2010 JL₃₃, none of which [except for (248590) 2006 CS, (436329) 2010 GX₆₂, (451124) 2009 KC₃ which produce southerly radiants that are difficult to detect for CMOR] has detectable meteor activity. On the other hand, the remaining three objects with detected showers (2004 TG₁₀, 2009 WN₂₅ and 2012 BU₆₁) are not selected by any of the surveys largely due to the lack of astrometric/physical observations, though the most recent NEOWISE catalog release includes the measurement for 2004 TG₁₀ (Nugent et al. 2015).

6. Conclusion

We conducted a direct survey for dormant comets in the ACO component in the NEO population. This was done by looking for meteor activity originated from each of the 407 NEOs as predicted by meteoroid stream models. This sample represents $\sim 80\%$ and $\sim 46\%$ of known NEOs in JFC-like orbits in the $H < 18$ and $H < 22$ population respectively.

To look for the virtual meteoroid streams predicted by the model, we analyzed 13 567 542 meteoroid orbits measured by the Canadian Meteor Orbit Radar (CMOR) in the interval of 2002–2016 using the wavelet technique developed by Galligan (2000) and Brown et al. (2008) and test the statistical significance of any detected association using a Monte Carlo subroutine. Among the 407 starting parent bodies, we found 36 virtual showers that are detectable by CMOR. Of these, we identify 5 positive detections that are statistically unlikely to be chance association. These include 3 previously known asteroid-stream associations [(196256) 2003 EH₁ – Quadrantids, 2004 TG₁₀ – Taurids, and 2009 WN₂₅ – November i Draconids], 1 new association (2012 BU₆₁ – Daytime ξ Sagittariids) and 1 new outburst detection [(139359) 2001 ME₁]. Except for the case of (139359) 2001 ME₁, which displayed only a single outburst in 2006, all other shower detections are in form of annual activity.

We also examined 32 previously proposed asteroid-shower associations. These associations were first checked with a Monte Carlo subroutine, from which we find only 8 associations are statistically significant. Excluding 3 associations that involve observational circumstances unfavorable for CMOR detection (e.g. southerly radiant or low arrival speed), 4 out of the remaining 5 associations involve showers that have only been reported by one study, while the last association [ψ Cassiopeiids – (5496) 1973 NA] involves some observation–model discrepancy. We leave these questions for future studies.

Based on the results above, we derive a lower limit to the dormant comet fraction of $2.0 \pm 1.7\%$ among all NEOs, slightly lower than previous numbers derived based on dynamical and physical considerations of the parent. This number must be taken with caution as we assume a median dust production from *known* JFC comets. The typical dust production of already-dead comets, however, is not truly known. A dormant comet fraction of $\sim 8\%$ as concluded by other studies would require a characteristic dust production about 10% of the median model. Another caveat is the possibility of overestimating the number of visible showers (hence, reducing the derived dormant comet fraction) due to very steep dust size distribution ($q \gg 3.6$), but this is not supported by cometary observations.

We also derive a dormancy rate of $\sim 10^{-5} \text{ yr}^{-1}$ per comet, consistent with previous model predictions and significantly lower than the observed and predicted disruption probability. This confirms disruption and dynamical removal as the dominant end state for near-Earth JFCs, while dormancy is relatively uncommon. We predict the existence of a significant number of “orphan” meteoroid streams where parents have been disrupted or dynamically removed. While it is challenging to investigate the formation of these streams in the absence of an observable parent, it might be possible to retrieve some knowledge of the parent based on meteor data alone.

We thank an anonymous referee for his/her careful review. We also thank Paul

Wiegert for comments and permission to use his computational resource, as well as Zbigniew Krzeminski, Jason Gill, Robert Weryk and Daniel Wong for helping with CMOR operations. This work was made possible by the facilities of the Shared Hierarchical Academic Research Computing Network (SHARCNET:www.sharcnet.ca) and Compute/Calcul Canada. Funding support from the NASA Meteoroid Environment Office (cooperative agreement NNX15AC94A) for CMOR operations is gratefully acknowledged.

A. Median Dust Production Model for Typical Jupiter-family Comets

To estimate the dust production of a typical Jupiter-family Comet (JFC), we compile the $Af\rho$ of 35 near-Earth JFCs from the Cometas-Obs database, using the measurements provided by various observers in the duration of 2009–2015. $Af\rho$ is an indicator of the dust product of a comet (c.f. A’Hearn et al. 1984, 1995) and is defined by

$$Af\rho = \frac{4r_h^2\Delta^2}{\rho} \frac{\mathcal{F}_C}{\mathcal{F}_\odot} \quad (\text{A1})$$

where r_h is the heliocentric distance of the comet in AU, Δ is the geocentric distance of the comet (in the same unit of ρ , typically in km or cm), and \mathcal{F}_C and \mathcal{F}_\odot are the fluxes of the comet within the field of view as observed by the observer and the Sun at a distance of 1 AU. The photometric aperture size, or $2\rho/\Delta$, is usually determined by the threshold value that the flux reaches an asymptote.

Since $Af\rho$ measurements are conducted at various r_h , we scale each $Af\rho$ measurement to $r_h = 1$ AU by

$$Af\rho_0 = Af\rho \cdot r_h^{4/3} \quad (\text{A2})$$

The $Af\rho_0$ number can be converted to the dust production rate at 1 AU following the derivation of Ye & Wiegert (2014):

$$N_d(a_1, a_2) = \frac{655A_1(a_1, a_2)Af\rho_0}{8\pi A_B\phi(\alpha)[A_3(a_1, a_2) + 1000A_{3.5}(a_1, a_2)]} \quad (\text{A3})$$

where $[a_1, a_2]$ is the size range of the meteoroids responsible for the detected flux where we use $a_1 = 10^{-5}$ m, $a_2 = 10^{-2}$ m, $A_x = (a_2^{x-s} - a_1^{x-s})/(x - s)$ for $x \neq s$ and $A_x = \ln a_2/a_1$ for $x = s$, with $s = 3.6$ being the size population index of the meteoroids (Fulle 2004), $A_B = 0.05$ is the Bond albedo and $\phi(\alpha)$ is the normalized phase function, which $\phi(\alpha) = 1$ for isotropic scattering. From Figure 6, we derive median $Af\rho_0$ to be 0.2 m, corresponding to a dust production rate of 7×10^{14} particles per orbit assuming an active time per orbit of ~ 1 yr.

B. Radiants, Activity Profiles and Dust Size Distributions of Predicted Virtual Showers

REFERENCES

- Abedin, A., Spurný, P., Wiegert, P., et al. 2015, *Icarus*, 261, 100
- A’Hearn, M. F., Millis, R. C., Schleicher, D. O., Osip, D. J., & Birch, P. V. 1995, *Icarus*, 118, 223
- A’Hearn, M. F., Schleicher, D. G., Millis, R. L., Feldman, P. D., & Thompson, D. T. 1984, *AJ*, 89, 579
- Andrejić, Ž., Šegon, D., Korlević, K., et al. 2013, WGN, Journal of the International Meteor Organization, 41, 103
- Babadzhanov, P. B., Kokhirova, G. I., & Obrubov, Y. V. 2015, *Solar System Research*, 49, 165
- Babadzhanov, P. B., & Obrubov, I. V. 1992, *Celestial Mechanics and Dynamical Astronomy*, 54, 111
- Babadzhanov, P. B., Williams, I. P., & Kokhirova, G. I. 2009, *A&A*, 507, 1067
- Belton, M. J. S. 2014, *Icarus*, 231, 168
- Binzel, R. P., Rivkin, A. S., Stuart, J. S., et al. 2004, *Icarus*, 170, 259
- Bottke, W. F., Morbidelli, A., Jedicke, R., et al. 2002, *Icarus*, 156, 399
- Bronshten, V. A. 1981, *Astronomicheskii Vestnik*, 15, 44
- Brown, P., Hocking, W. K., Jones, J., & Rendtel, J. 1998, *MNRAS*, 295, 847
- Brown, P., & Jones, J. 1998, *Icarus*, 133, 36
- Brown, P., Weryk, R. J., Wong, D. K., & Jones, J. 2008, *Icarus*, 195, 317

- Brown, P., Wong, D. K., Weryk, R. J., & Wiegert, P. 2010, *Icarus*, 207, 66
- Bruzzone, J. S., Brown, P., Weryk, R. J., & Campbell-Brown, M. D. 2015, *MNRAS*, 446, 1625
- Campbell-Brown, M. D., & Koschny, D. 2004, *A&A*, 418, 751
- Cepplecha, Z., Borovička, J., Elford, W. G., et al. 1998, *Space Sci. Rev.*, 84, 327
- Chambers, J. E. 1999, *MNRAS*, 304, 793
- Chambers, J. E., & Migliorini, F. 1997, in *Bulletin of the American Astronomical Society*, Vol. 29, AAS/Division for Planetary Sciences Meeting Abstracts #29, 1024
- Cremonese, G., Fulle, M., Marzari, F., & Vanzani, V. 1997, *A&A*, 324, 770
- de León, J., Campins, H., Tsiganis, K., Morbidelli, A., & Licandro, J. 2010, *A&A*, 513, A26
- DeMeo, F., & Binzel, R. P. 2008, *Icarus*, 194, 436
- Di Sisto, R. P., Fernández, J. A., & Brunini, A. 2009, *Icarus*, 203, 140
- Drummond, J. D. 1981, *Icarus*, 45, 545
- Everhart, E. 1985, in *Dynamics of Comets: Their Origin and Evolution*, Proceedings of IAU Colloq. 83, held in Rome, Italy, June 11-15, 1984. Edited by Andrea Carusi and Giovanni B. Valsecchi. Dordrecht: Reidel, *Astrophysics and Space Science Library*. Volume 115, 1985, p.185, ed. A. Carusi & G. B. Valsecchi, 185
- Fernández, J. A., Gallardo, T., & Brunini, A. 2002, *Icarus*, 159, 358
- Fernández, Y. R., Jewitt, D. C., & Sheppard, S. S. 2005, *AJ*, 130, 308
- Fernández, Y. R., McFadden, L. A., Lisse, C. M., Helin, E. F., & Chamberlin, A. B. 1997, *Icarus*, 128, 114

- Fulle, M. 2004, Motion of cometary dust, ed. G. W. Kronk, 565–575
- Galligan, D. P. 2000, PhD thesis, University of Canterbury
- . 2001, MNRAS, 327, 623
- Gartrell, G., & Elford, W. G. 1975, Australian Journal of Physics, 28, 591
- Göckel, C., & Jehn, R. 2000, MNRAS, 317, L1
- Greenstreet, S., Ngo, H., & Gladman, B. 2012, Icarus, 217, 355
- Hartogh, P., Lis, D. C., Bockelée-Morvan, D., et al. 2011, Nature, 478, 218
- Hoffmeister, C. 1948, Meteorstrome. Meteoric currents.
- Jedicke, R., Granvik, M., Micheli, M., et al. 2015, ArXiv e-prints, arXiv:1503.04272
- Jenniskens, P. 2004, AJ, 127, 3018
- . 2006, Meteor Showers and their Parent Comets
- . 2008, Earth Moon and Planets, 102, 505
- Jenniskens, P., & Vaubaillon, J. 2010, AJ, 139, 1822
- Jenniskens, P., Nénon, Q., Albers, J., et al. 2016, Icarus, 266, 331
- Jewitt, D., & Li, J. 2010, AJ, 140, 1519
- Jewitt, D., Li, J., & Agarwal, J. 2013, ApJ, 771, L36
- Jewitt, D., Weaver, H., Agarwal, J., Mutchler, M., & Drahus, M. 2010, Nature, 467, 817
- Jones, D. C., Williams, I. P., & Porubčan, V. 2006, MNRAS, 371, 684
- Jones, J. 1995, MNRAS, 275, 773

- Jones, J., Brown, P., Ellis, K. J., et al. 2005, *Planet. Space Sci.*, 53, 413
- Jones, W. 1997, *MNRAS*, 288, 995
- Kashcheyev, B. L., & Lebedinets, V. N. 1967, *Smithsonian Contributions to Astrophysics*, 11, 183
- Kim, Y., Ishiguro, M., & Usui, F. 2014, *ApJ*, 789, 151
- Kokhirova, G. I., & Babadzhanov, P. B. 2015, *Meteoritics and Planetary Science*, 50, 461
- Kornoš, L., Matlovič, P., Rudawska, R., et al. 2014, *Meteoroids 2013*, 225
- Kresak, L. 1979, *Dynamical interrelations among comets and asteroids*, ed. T. Gehrels, 289–309
- Licandro, J., Alí-Lagoa, V., Tancredi, G., & Fernández, Y. 2016, *A&A*, 585, A9
- Lindblad, B. A. 1971, *Smithsonian Contributions to Astrophysics*, 12, 14
- Luu, J., & Jewitt, D. 1990, *Icarus*, 86, 69
- Mainzer, A., Grav, T., Bauer, J., et al. 2011, *ApJ*, 743, 156
- Marsden, B. G., Sekanina, Z., & Everhart, E. 1978, *AJ*, 83, 64
- McIntosh, B. A., & Hajduk, A. 1983, *MNRAS*, 205, 931
- Micheli, M., Tholen, D. J., & Jenniskens, P. 2016, *Icarus*, 267, 64
- Mommert, M., Harris, A. W., Mueller, M., et al. 2015, *AJ*, 150, 106
- Moorhead, A. V. 2016, *MNRAS*, 455, 4329
- Murray, C. D., & Dermott, S. F. 1999, *Solar system dynamics*

- Nilsson, C. S. 1964, *Australian Journal of Physics*, 17, 205
- Nugent, C. R., Mainzer, A., Masiero, J., et al. 2015, *ApJ*, 814, 117
- Olsson-Steel, D. 1987, *Australian Journal of Astronomy*, 2, 21
- Pauls, A., & Gladman, B. 2005, *Meteoritics and Planetary Science*, 40, 1241
- Porubcan, V., & Gavajdova, M. 1994, *Planet. Space Sci.*, 42, 151
- Porubcan, V., Stohl, J., & Vana, R. 1992, in *Asteroids, Comets, Meteors 1991*, ed. A. W. Harris & E. Bowell
- Porubčan, V., Kornoš, L., & Williams, I. P. 2006, *Contributions of the Astronomical Observatory Skalnaté Pleso*, 36, 103
- Rubincam, D. P. 2000, *Icarus*, 148, 2
- Schiaparelli, G. V. 1866, *Intorno AL corso ed all’ origine probabile delle stelle meteoriche*
- . 1867, *Note E riflessioni intorno alla teoria astronomica delle stelle cadenti*
- Sekanina, Z. 1973, *Icarus*, 18, 253
- . 1976, *Icarus*, 27, 265
- Southworth, R. B., & Hawkins, G. S. 1963, *Smithsonian Contributions to Astrophysics*, 7, 261
- Steel, D. I., Asher, D. J., & Clube, S. V. M. 1991, *MNRAS*, 251, 632
- Stuart, J. S. 2001, *Science*, 294, 1691
- Tancredi, G. 1995, *A&A*, 299, 288
- . 2014, *Icarus*, 234, 66

- Taylor, P. A., Margot, J.-L., Vokrouhlický, D., et al. 2007, *Science*, 316, 274
- Terentjeva, A. K. 1989, *WGN, Journal of the International Meteor Organization*, 17, 242
- Tisserand, F. 1891, *Traité de mécanique céleste* (Gauthier-Villars)
- Šegon, D., Andreić, Ž., Gural, P., et al. 2014a, *WGN, Journal of the International Meteor Organization*, 42, 227
- Šegon, D., Andreić, Ž., Korlević, K., & Vida, D. 2015, in *Proceedings of the International Meteor Conference Mistelbach, Austria, 27-30 August 2015*, ed. J.-L. Rault & P. Roggemans, 51–57
- Šegon, D., Gural, P., Andreić, Ž., et al. 2014b, *WGN, Journal of the International Meteor Organization*, 42, 57
- Vaubaillon, J., Colas, F., & Jorda, L. 2005, *A&A*, 439, 761
- Weissman, P. R., Bottke, Jr., W. F., & Levison, H. F. 2002, *Asteroids III*, 669
- Weryk, R. J., & Brown, P. G. 2012, *Planet. Space Sci.*, 62, 132
- . 2013, *Planet. Space Sci.*, 81, 32
- Wiegert, P., & Brown, P. 2004, *Earth Moon and Planets*, 95, 19
- Wiegert, P., & Tremaine, S. 1999, *Icarus*, 137, 84
- Wiegert, P., Vaubaillon, J., & Campbell-Brown, M. 2009, *Icarus*, 201, 295
- Williams, I. P., & Wu, Z. 1993, *MNRAS*, 262, 231
- Ye, Q., Brown, P. G., Campbell-Brown, M. D., & Weryk, R. J. 2013, *MNRAS*, 436, 675
- Ye, Q., & Wiegert, P. A. 2014, *MNRAS*, 437, 3283

- Ye, Q., Wiegert, P. A., Brown, P. G., Campbell-Brown, M. D., & Weryk, R. J. 2014, MNRAS, 437, 3812
- Ye, Q.-Z., Brown, P. G., Bell, C., et al. 2015, ApJ, 814, 79
- Ye, Q.-Z., Brown, P. G., & Wiegert, P. A. 2016a, ApJ, 818, L29
- Ye, Q.-Z., & Hui, M.-T. 2014, ApJ, 787, 115
- Ye, Q.-Z., Hui, M.-T., Brown, P. G., et al. 2016b, Icarus, 264, 48
- Yeomans, D. K., Yau, K. K., & Weissman, P. R. 1996, Icarus, 124, 407

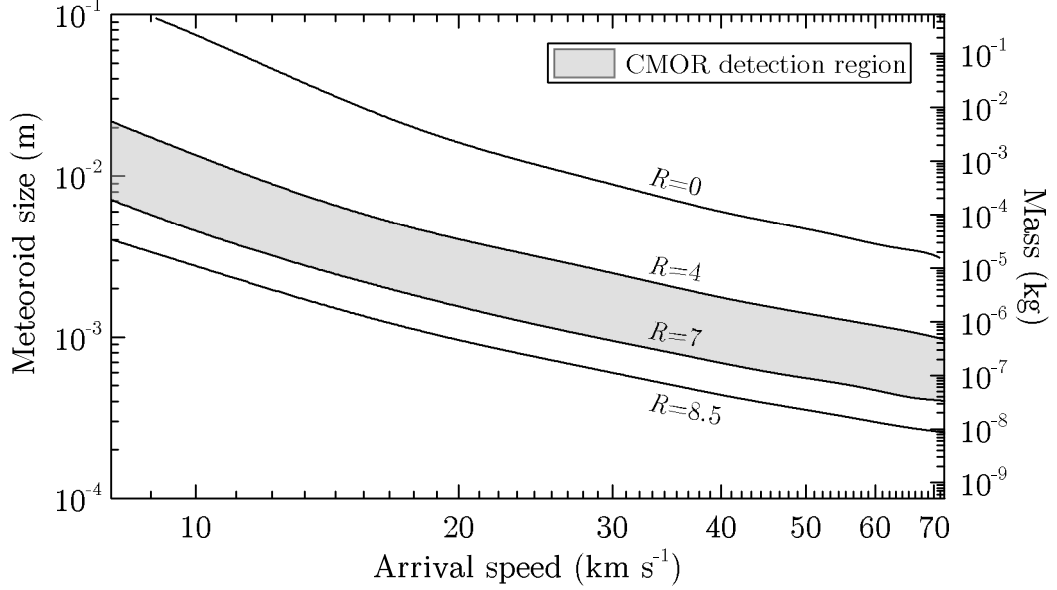


Fig. 1.— Size-speed relation of meteors at absolute magnitude in the general R bandpass of $R = 0$ (typical detection limit of all-sky video networks), $R = 4$ (typical detection limit of narrow field video networks, as well as the upper limit of automated radar detection as meteor echo scattering changes from the underdense to the overdense regime, c.f. Ye et al. 2014), $R = 7$ (CMOR median for meteor orbits) and $R = 8.5$ (CMOR detection limit) assuming bulk density of 1000 kg m^{-3} . Calculated using the meteoroid ablation model developed by Campbell-Brown & Koschny (2004), where the luminous efficiency is constant at 0.7% and the ionization coefficient is from Bronshten (1981). Note that other authors (Jones 1997; Weryk & Brown 2013) have argued that these coefficients may be off by up to a factor of ~ 10 at extreme speeds ($v_g \lesssim 15 \text{ km s}^{-1}$ or $v_g \gtrsim 70 \text{ km s}^{-1}$), but most of the showers we examined in this work have moderate v_g , hence this issue does not impact our final results. The CMOR detection range is appropriated to an ionization coefficient I of 5–100 in Wiegert et al. (2009)’s model.

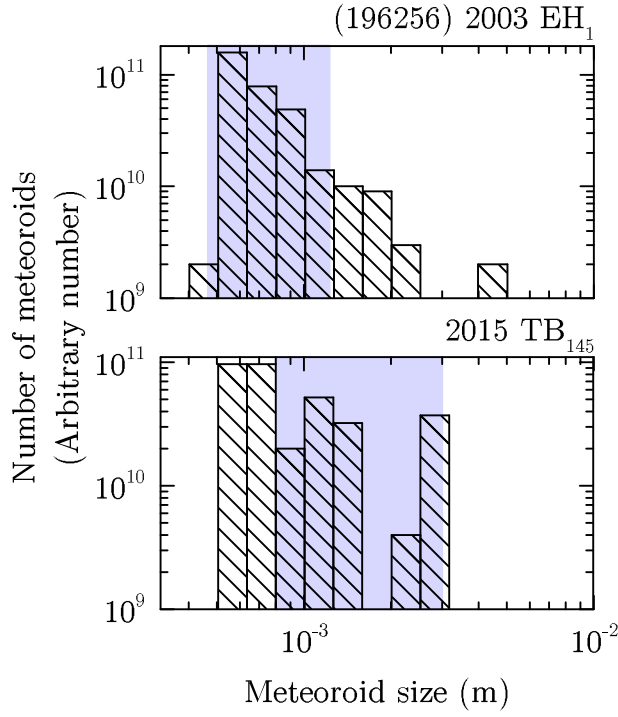


Fig. 2.— Examples of altered arrival size distribution due to different delivery efficiency at different sizes. The meteoroids from (196256) 2003 EH₁ (top figure) is more similar to the original size distribution at the parent, while for the case of 2015 TB₁₄₅ (lower figure), larger meteoroids are more efficiently delivered than smaller meteoroids. Shaded areas are the CMOR-detection size range.

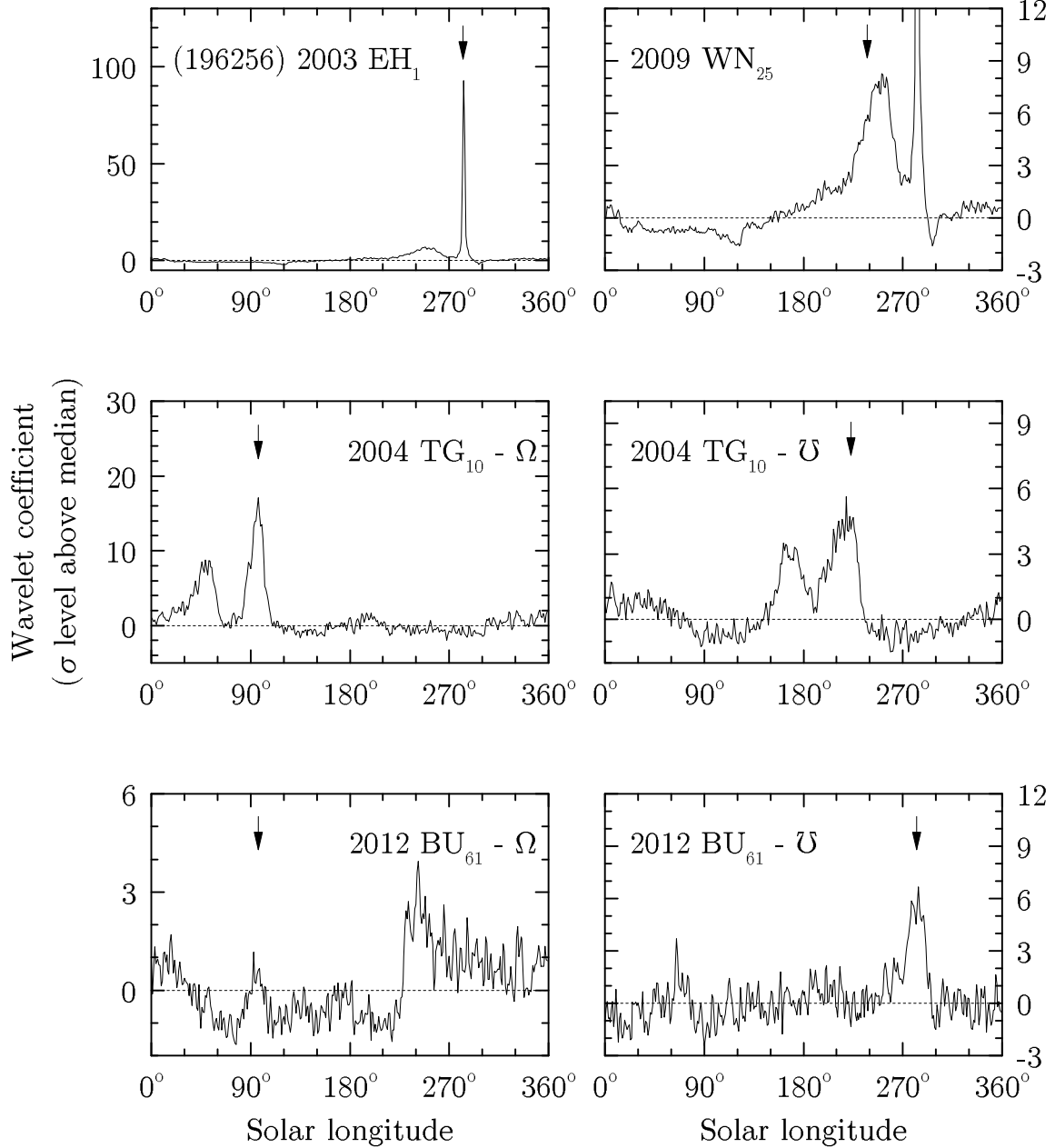


Fig. 3.— Detection of annual meteor activity that may be associated with (196256) 2003 EH₁, 2004 TG₁₀ (both ascending node Ω and descending node Ū), 2009 WN₂₅, 2011 BE₃₈ and 2012 BU₆₁ (both ascending node Ω and descending node Ū). Activity peaks are highlighted by arrows. The figures show the relative wavelet coefficients at radiant given in each graph in units of the numbers of standard deviations above the annual median.

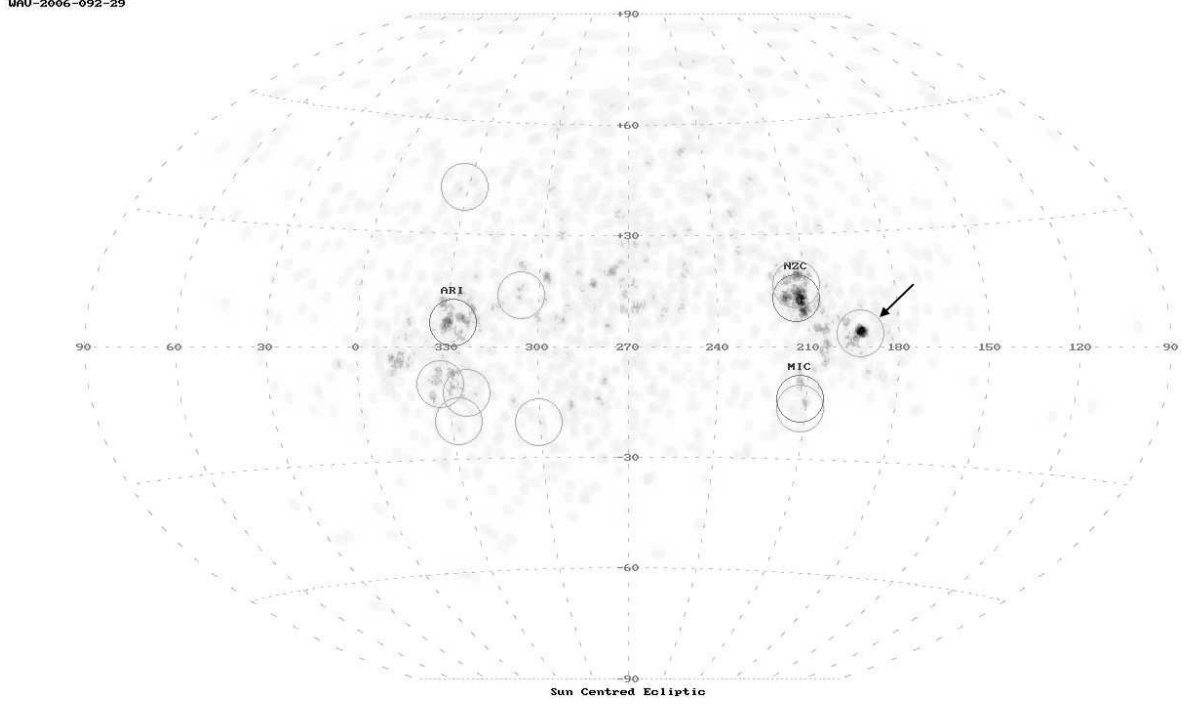


Fig. 4.— Possible activity from (139359) 2001 ME₁ on 2006 Jun. 24 in sun-centered ecliptic sphere. Darker contour corresponds to areas in the sky with denser radiants. Known showers are marked by dark circles and the International Astronomical Union (IAU) shower designation (ARI = Arietids, NZC = Northern June Aquilids, MIC = Microscopiids). Unknown enhancements are marked by gray circles. Note that most enhancements are random fluctuations. The possible activity associated with (139359) 2001 ME₁ is the strong enhancement near $\lambda - \lambda_{\odot} = 190^{\circ}$, $\beta = +5^{\circ}$.

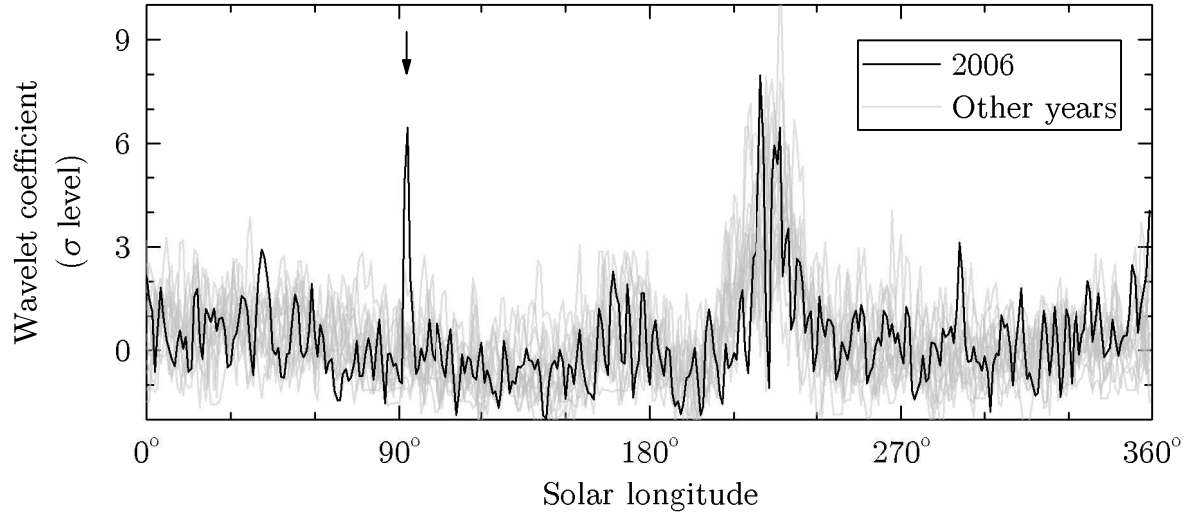


Fig. 5.— Variation of the wavelet coefficient at $\lambda - \lambda_{\odot} = 191^{\circ}$, $\beta = +4^{\circ}$ and $v_g = 30.0 \text{ km s}^{-1}$ in 2002–2015 (gray lines except for 2006). Possible activity from (139359) 2001 ME₁ in 2006 is marked by an arrow. Recurring activity around $\lambda_{\odot} = 220^{\circ}$ is from the Taurids complex in November.

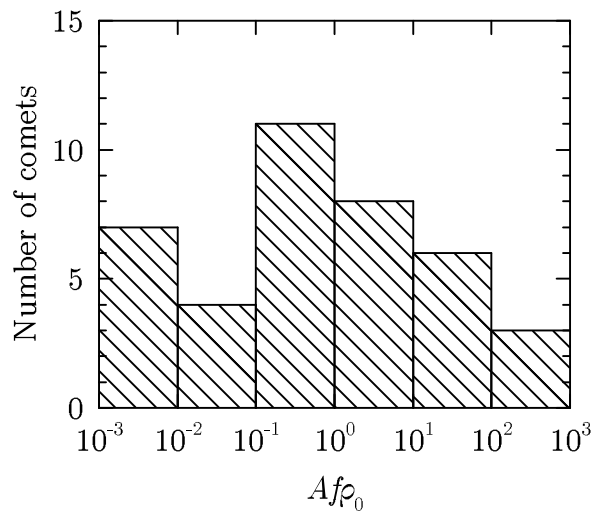


Fig. 6.— Distribution of $Af\rho_0$ of a number of near-Earth JFCs. The median $Af\rho_0$ is 0.2 m, corresponding to a dust production rate of 7×10^{14} meteoroids (appropriated to the size range of 0.5–50 mm) per orbit.

Table 1. Objects that are capable to produce CMOR-detectable annual meteor activities. Listed are the properties of the parent (absolute magnitude H , Tisserand parameter with respect to Jupiter, T_J , Minimum Orbit Intersection Distance (MOID) with respect to the Earth, orbital chaotic timescale τ_{parent}), dynamical properties of the hypothetical meteoroid stream (stream age τ_{stream} , encircling time τ_{enc}), and calculated meteor activities at ascending node Ω and/or descending node Υ (including the time of activity in solar longitude λ_{\odot} , radiant in J2000 sun-centered ecliptic coordinates, $\lambda - \lambda_{\odot}$ and β , radiant size σ_{rad} , geocentric speed v_g , and meteoroid flux \mathcal{F} derived from median JFC model.

Parent	Parent				Stream								
	H	MOID (AU)	T_J	τ_{parent} (yr)	τ_{stream} (yr)	τ_{enc} (yr)	Node	λ_{\odot}	$\lambda - \lambda_{\odot}$	β	σ_{rad}	v_g (km s $^{-1}$)	$\mathcal{F}_{\text{CMOR}}$ (km $^{-2}$ hr $^{-1}$)
(3360) Syrinx	15.9	0.108	2.965	5400	4650	500	Υ	$212^{\circ} \pm 2^{\circ}$	357°	$+23^{\circ}$	$\pm 1^{\circ}$	24.9 ± 0.3	0.001
(16960) 1998 QS ₅₂	14.3	0.015	3.000	> 10000	10000	100	Ω	$83^{\circ} \pm 1^{\circ}$	344°	-13°	$\pm 1^{\circ}$	30.8 ± 0.1	2.651
(137427) 1999 TF ₂₁₁	15.2	0.020	2.968	5300	550	200	Υ	$348^{\circ} \pm 1^{\circ}$	345°	$+81^{\circ}$	$\pm 1^{\circ}$	24.2 ± 0.2	0.002
(139359) 2001 ME ₁	16.6	0.012	2.674	4900	700	200	Υ	$92^{\circ} \pm 2^{\circ}$	191°	$+4^{\circ}$	$\pm 1^{\circ}$	29.9 ± 0.3	0.021
(192642) 1999 RD ₃₂	16.3	0.050	2.872	2500	800	100	Ω	$155^{\circ} \pm 3^{\circ}$	2°	-9°	$\pm 1^{\circ}$	22.8 ± 0.6	0.001
(196256) 2003 EH ₁	16.2	0.212	2.065	1300	300	200	Υ	$283^{\circ} \pm 1^{\circ}$	275°	$+63^{\circ}$	$\pm 1^{\circ}$	41.6 ± 0.2	0.012
(247360) 2001 XU	19.2	0.005	2.749	> 10000	6700	100	Υ	$262^{\circ} \pm 1^{\circ}$	191°	$+17^{\circ}$	$\pm 1^{\circ}$	29.1 ± 0.2	0.773
(248590) 2006 CS	16.5	0.105	2.441	2000	1800	200	Ω	$352^{\circ} \pm 1^{\circ}$	305°	-77°	$\pm 1^{\circ}$	30.6 ± 0.4	0.419
(297274) 1996 SK	16.8	0.004	2.968	2200	1250	200	Υ	$204^{\circ} \pm 3^{\circ}$	184°	$+2^{\circ}$	$\pm 1^{\circ}$	24.4 ± 0.6	0.009
(307005) 2001 XP ₁	18.0	0.016	2.560	> 10000	10000	200	Υ	$268^{\circ} \pm 1^{\circ}$	191°	$+50^{\circ}$	$\pm 1^{\circ}$	28.5 ± 0.0	0.781
(399457) 2002 PD ₄₃	19.1	0.029	2.439	> 10000	300	300	Ω	$130^{\circ} \pm 3^{\circ}$	334°	-8°	$\pm 1^{\circ}$	39.1 ± 0.6	0.002
(401857) 2000 PG ₃	16.1	0.210	2.550	3200	2150	100	Ω	$176^{\circ} \pm 2^{\circ}$	192°	-12°	$\pm 1^{\circ}$	30.2 ± 0.3	0.006
(436329) 2010 GX ₆₂	20.1	0.014	2.756	> 10000	600	200	Ω	$25^{\circ} \pm 2^{\circ}$	19°	-50°	$\pm 2^{\circ}$	18.7 ± 0.3	0.003
(442037) 2010 PR ₆₆	19.3	0.002	2.818	2800	1200	200	Ω	$114^{\circ} \pm 4^{\circ}$	25°	-40°	$\pm 4^{\circ}$	16.4 ± 0.2	0.001
(451124) 2009 KC ₃	18.0	0.006	2.728	4300	900	700	Ω	$162^{\circ} \pm 2^{\circ}$	46°	-31°	$\pm 2^{\circ}$	12.6 ± 0.3	0.001
1999 LT ₁	17.6	0.095	2.586	2100	1800	200	Υ	$67^{\circ} \pm 1^{\circ}$	343°	$+78^{\circ}$	$\pm 1^{\circ}$	25.9 ± 0.5	0.544
2001 HA ₄	17.7	0.018	2.772	> 10000	4250	200	Ω	$179^{\circ} \pm 2^{\circ}$	184°	-20°	$\pm 1^{\circ}$	25.0 ± 0.2	0.122

Table 1—Continued

Parent	Parent				Stream								
	H	MOID (AU)	T_J	τ_{parent} (yr)	τ_{stream} (yr)	τ_{enc} (yr)	Node	λ_{\odot}	$\lambda - \lambda_{\odot}$	β	σ_{rad}	v_g (km s $^{-1}$)	$\mathcal{F}_{\text{CMOR}}$ (km $^{-2}$ hr $^{-1}$)
2003 CG ₁₁	20.5	0.018	2.900	> 10000	7200	200	♊	134° ± 2°	1°	+30°	±1°	22.9 ± 0.2	0.057
2003 OV	18.3	0.082	2.987	> 10000	6300	100	♋	108° ± 4°	194°	−5°	±1°	30.0 ± 0.8	0.015
..	♊	346° ± 4°	346°	+5°	±1°	29.5 ± 0.9	0.008
2004 BZ ₇₄	18.1	0.032	2.369	7900	3750	100	♋	60° ± 1°	192°	−11°	±1°	32.0 ± 0.2	0.044
2004 CK ₃₉	19.2	0.068	2.991	> 10000	9350	150	♋	197° ± 3°	348°	−11°	±1°	29.1 ± 0.4	0.002
..	♊	334° ± 2°	191°	+11°	±1°	29.1 ± 0.4	0.010
2004 TG ₁₀	19.4	0.022	2.992	6600	6100	400	♋	102° ± 2°	346°	−3°	±1°	30.1 ± 0.6	0.094
..	♊	223° ± 3°	194°	+3°	±1°	30.0 ± 0.5	0.065
2005 FH	17.7	0.038	2.821	6200	8100	150	♋	328° ± 2°	3°	−58°	±2°	22.5 ± 0.2	0.012
2005 UN ₁₅₇	18.2	0.420	2.581	6000	3750	200	♋	175° ± 2°	339°	−13°	±1°	36.4 ± 0.4	0.008
..	♊	261° ± 3°	203°	+13°	±1°	36.9 ± 0.5	0.003
2005 WY ₅₅	20.7	0.004	3.042	4700	2500	1200	♋	70° ± 3°	7°	−12°	±1°	19.6 ± 0.6	0.012
2006 AL ₈	18.4	0.056	2.159	2900	7300	100	♊	312° ± 2°	339°	+24°	±1°	36.0 ± 0.4	0.013
2006 KK ₂₁	20.4	0.033	2.605	5000	4000	100	♋	51° ± 2°	347°	−11°	±1°	30.5 ± 0.4	0.022
..	♊	180° ± 2°	192°	+10°	±1°	30.2 ± 0.3	0.031
2007 CA ₁₉	17.6	0.019	2.679	4300	300	100	♋	354° ± 1°	185°	−10°	±1°	27.1 ± 0.2	0.018
..	♊	190° ± 1°	355°	+10°	±1°	27.0 ± 0.1	0.010
2008 SV ₁₁	18.4	0.018	2.957	8400	3300	200	♊	8° ± 4°	10°	+15°	±3	18.6 ± 0.5	0.005
2008 YZ ₂₈	20.0	0.094	2.969	3300	4000	200	♊	270° ± 6°	358°	+54°	±5	23.8 ± 0.4	0.001
2009 HD ₂₁	18.2	0.015	2.881	6900	1400	100	♊	180° ± 3°	20°	+41°	±3	17.7 ± 0.2	0.005

Table 1—Continued

Parent	Parent				Stream								
	H	MOID (AU)	T_J	τ_{parent} (yr)	τ_{stream} (yr)	τ_{enc} (yr)	Node	λ_{\odot}	$\lambda - \lambda_{\odot}$	β	σ_{rad}	v_g (km s $^{-1}$)	$\mathcal{F}_{\text{CMOR}}$ (km $^{-2}$ hr $^{-1}$)
2009 SG ₁₈	17.8	0.025	2.313	8500	9250	200	\mathfrak{U}	$177^\circ \pm 1^\circ$	237°	$+70^\circ$	$\pm 1^\circ$	34.1 ± 0.3	0.172
2009 WN ₂₅	18.4	0.114	1.959	2700	100	400	\mathfrak{U}	$232^\circ \pm 1^\circ$	271°	$+63^\circ$	$\pm 1^\circ$	41.7 ± 0.1	1.034
2010 JL ₃₃	17.7	0.033	2.910	4100	4000	100	Ω	$250^\circ \pm 5^\circ$	10°	-8°	$\pm 2^\circ$	19.0 ± 1.1	0.001
2010 XC ₁₁	18.7	0.030	2.792	6400	850	700	Ω	$282^\circ \pm 2^\circ$	192°	-7°	$\pm 1^\circ$	29.9 ± 0.4	0.002
2011 GH ₃	18.5	0.149	3.020	8600	6850	200	Ω	$237^\circ \pm 1^\circ$	357°	-9°	$\pm 1^\circ$	24.6 ± 0.2	0.011
..	\mathfrak{U}	$49^\circ \pm 1^\circ$	183°	$+9^\circ$	$\pm 1^\circ$	24.7 ± 0.2	0.013
2011 GN ₄₄	18.3	0.009	2.922	> 10000	10000	200	Ω	$196^\circ \pm 1^\circ$	318°	-65°	$\pm 1^\circ$	32.6 ± 0.1	5.829
2012 BU ₆₁	21.3	0.027	2.933	8400	1700	1100	Ω	$101^\circ \pm 4^\circ$	180°	-6°	$\pm 1^\circ$	23.1 ± 0.9	0.002
..	\mathfrak{U}	$280^\circ \pm 4^\circ$	359°	$+6^\circ$	$\pm 1^\circ$	23.5 ± 1.0	0.001
2012 FZ ₂₃	18.2	0.020	2.367	4400	1250	200	Ω	$359^\circ \pm 1^\circ$	269°	-61°	$\pm 1^\circ$	41.7 ± 0.2	0.369
2012 HG ₈	19.7	0.004	2.967	4000	2800	100	\mathfrak{U}	$215^\circ \pm 4^\circ$	182°	$+36^\circ$	± 3	23.7 ± 0.3	0.013
2012 TO ₁₃₉	19.7	0.001	2.759	4800	300	100	Ω	$290^\circ \pm 4^\circ$	196°	-4°	$\pm 1^\circ$	33.1 ± 0.8	0.001
..	\mathfrak{U}	$179^\circ \pm 1^\circ$	345°	$+3^\circ$	$\pm 1^\circ$	32.6 ± 0.1	0.196
2015 TB ₁₄₅	19.9	0.002	2.964	> 10000	10000	100	Ω	$217^\circ \pm 1^\circ$	204°	-24°	$\pm 1^\circ$	34.9 ± 0.2	1.738

Table 2. Orbits and radiant characteristics of the possible meteor activity associated with 2009 WN₂₅, 2011 BE₃₈ and 2012 BU₆₁. Listed are perihelion distance q , eccentricity e , inclination i , longitude of ascending node Ω and argument of perihelion ω for the parent (taken from JPL 31, 28 and 15 for the respective parent) and the meteor shower from the given reference. The uncertainties in the orbital elements for the parents are typically in the order of 10^{-5} to 10^{-8} in their respective units and are not shown. Epochs are in J2000. Shwon are the absolute magnitude of the parent as well as the expected number of NEOs with $H < 18$ and $H < 22$ which are expected to have $D' < D'_0$ relative to that of the proposed parent. Values of $\langle X \rangle$ near or larger than 1 suggest that the association is not statistically significant.

	Orbital elements (J2000)					Geocentric radiant (J2000)			$\langle X \rangle$	
	q (AU)	e	i	Ω	ω	$\lambda - \lambda_\odot$	β	v_g (km s ⁻¹)	$H < 18$	$H < 22$
2009 WN ₂₅ ($H = 18.4$) – November i Draconids										
2009 WN ₂₅	1.10238	0.66278	71.986°	232.086°	180.910°	271°	+63°	41.7		
						±1°	±1°	±0.1		
Shower prediction – this work	0.987	0.619	73.6°	238.0°	184.6°	267.6°	+62.0°	41.4	0.001–0.05	0.02–0.6
	±0.002	±0.133	7 ± 2.3°	±0.5°	±2.9°	±0.1°	±0.1°	±0.1		
Observed shower – Brown et al. (2010)	0.9874	0.737	74.9°	241.0°	181.09°	270.1°	+62.5°	43	0.003	0.04
Observed shower – Jenniskens et al. (2016)	0.973	0.734	72.9°	254.4°	194.7°	260.9°	+63.2°	41.9	0.4	6
2002 AU ₅ ($H = 17.8$) & 2012 BU ₆₁ ($H = 21.5$) – Daytime ξ Sagittariids (XSA) & Daytime Scutids (JSC) ^b										
2002 AU ₅	0.40301	0.75531	9.256°	354.989°	21.261°	359°	+6°	23.5		
						±1°	±1°	±1.0		
2012 BU ₆₁	0.55333	0.78023	5.277°	297.700°	72.461°	359°	+6°	23.5		
						±1°	±1°	±1.0		
XSA prediction – this work	0.46	0.77	5.9°	291.0°	76.6°	352.6°	+6.4°	25.2	AU ₅ : 0.8–1.2	AU ₅ : 10–15
	±0.02	±0.04	±1.0°	±0.5°	±2.1°	±0.1°	±0.1°	±0.1	BU ₆₁ : 0.05–0.2	BU ₆₁ : 0.6–2
XSA observation – Sekanina (1976)	0.29	0.74	1.1°	304.9°	46.9°	338.0°	+0.9°	24.4	AU ₅ : 12–13	AU ₅ : 156–164
	±0.01	±0.02	±0.7°	±1.4°	±1.8°	±1.0°	±0.6°		BU ₆₁ : 8–10	BU ₆₁ : 101–126

Table 2—Continued

Orbital elements (J2000)					Geocentric radiant (J2000)			$\langle X \rangle$	
q	e	i	Ω	ω	$\lambda - \lambda_{\odot}$	β	v_{g}	$H < 18$	$H < 22$
(AU)							(km s ⁻¹)		

^aAscending node.

^bDescending node.

Table 3. Previously proposed associations that are not reproduced in this work. Only objects that are in our initial 407-object list are included. “Established showers” means confirmed meteor showers in the IAU catalog, not established parent-shower linkages (likewise for unestablished showers). Listed are the absolute magnitude of the parent H , sources where the linkage was proposed, orbital elements, and $\langle X \rangle$ for the NEO population of $H < 18$ and $H < 22$.

Shower	Proposed parent	H	Reference	$\langle X \rangle_{H<18}$	$\langle X \rangle_{H<22}$
Established showers:					
Corvids	(14827) Hypnos	18.3	O87, J16, JPL 49	1.4	18
..	(374038) 2004 HW	17.0	Je06, J16, JPL 60	0.1	1.4
Daytime April Piscids	2003 MT ₉	18.6	B09, B10, JPL 37	0.9	11
..	(401857) 2000 PG ₃ ^a	16.1	B09, B10, JPL 43	34	432
..	2002 JC ₉ ^a	18.5	B09, B10, JPL 26	10	121
κ Cygnids	(153311) 2001 MG ₁	17.2	Jo06, J16, JPL 63	0.8	10
..	(361861) 2008 ED ₆₉	17.0	J08, J16, JPL 36	1.7	21
Northern ι Aquariids	2003 MT ₉	18.6	B09, J16, JPL 37	9	114
ψ Cassiopeiids	(5496) 1973 NA	16.0	P92, J16, JPL 51	0.2	1.9

Unestablished showers:

66 Draconids	2001 XQ	19.2	S14a, JPL 14	0.003	0.04
August θ Aquillids	2004 MB ₆	19.5	K14, K15, JPL 17	16	203

Table 3—Continued

Shower	Proposed parent	H	Reference	$\langle X \rangle_{H<18}$	$\langle X \rangle_{H<22}$
Daytime ϵ Aquariids	(206910) 2004 NL ₈	17.1	G75, Je06, JPL 108	7	89
Daytime δ Scorpiids	2003 HP ₃₂ ^b	19.6	N64, B15, JPL 17	0.6	8
..	2007 WY ₃ ^b	18.2	N64, B15, JPL 18	6	75
δ Mensids	(248590) 2006 CS	16.5	Je06, JPL 48	0.001	0.02
η Virginids	2007 CA ₁₉	17.6	B15, J16, JPL 56	3.3	42
γ Piscids	6344 P-L	20.4	T89, Je06, JPL 16	51	648
γ Triangulids	2002 GZ ₈	18.2	P94, Je06, JPL 33	3.1	39
ι Cygnids	2001 SS ₂₈₇	18.3	A13, JPL 21	0.1	1.2
κ Cepheids	2009 SG ₁₈	17.8	S15, JPL 22	0.0004	0.006
λ Cygnids	(189263) 2005 CA	15.6	T89, Je06, JPL 51	15	185
Northern δ Leonids	(192642) 1999 RD ₃₂	16.3	L71, Je06, JPL 125	0.7	9
Northern δ Piscids	(401857) 2000 PG ₃ ^a	16.1	B09, J16, JPL 43	24	302
..	2002 JC ₉ ^a	18.5	B09, J16, JPL 26	8	107
Northern γ Virginids	2002 FC	18.9	T89, Je06, JPL 52	0.2	2.2

Table 3—Continued

Shower	Proposed parent	H	Reference	$\langle X \rangle_{H<18}$	$\langle X \rangle_{H<22}$
Northern σ Sagittariids ^c	(139359) 2001 ME ₁	16.6	S76, Je06, JPL 71	2.3	29
Southern α Leonids	(172678) 2003 YM ₁₃₇	18.7	Je06, JPL 51	13	166
Southern δ Piscids	(401857) 2000 PG ₃ ^a	16.1	B09, J16, JPL 43	15	195
..	2002 JC ₉ ^a	18.5	B09, J16, JPL 26	20	251
Southern ι Aquariids	2003 MT ₉	18.6	B08, B09, JPL 37	0.6	7
ζ^1 Cancrids	2012 TO ₁₃₉	19.7	S14b, JPL 13	0.08	1.0

Note. — Abbreviation of references: A13 – Andreić et al. (2013); B08 – Brown et al. (2008); B09 – Babadzhanov et al. (2009); B10 – Brown et al. (2010); B15 – Babadzhanov et al. (2015); G75 – Gartrell & Elford (1975); Je06 – Jenniskens (2006); Jo06 – Jones et al. (2006); J08 – Jenniskens (2008); J16 – Jenniskens et al. (2016); K14 – Kornoš et al. (2014); K15 – Kokhirova & Babadzhanov (2015); K67 – Kashcheyev & Lebedinets (1967); L71 – Lindblad

(1971); N64 – Nilsson (1964); O87 – Olsson-Steel (1987); P92 – Porubcan et al. (1992); Porubcan & Gavajdova (1994); S14a – Šegon et al. (2014b); S14b – Šegon et al. (2014a); S76 – Sekanina (1976); T89 – Terentjeva (1989)

^aObjects/streams thought be belonged to the same complex.

^bObjects/streams thought be belonged to the same complex.

^cCalled σ Carpricornids in Sekanina (1976).

Table 4. Predicted meteor outbursts from virtual young meteoroid trails from the shower parents. Shown are the age of the trail, period of expected activity (in date and solar longitude, λ_{\odot} , rounded to the nearest 1° solar longitude), radiant (in J2000 sun-centered ecliptic coordinates, $\lambda - \lambda_{\odot}$ and β), geocentric speed (v_g), and estimated meteoroid flux derived from median JFC model.

Parent	τ_{enc} (yr)	Date (UT)	Ejection	λ_{\odot}	$\lambda - \lambda_{\odot}$	β	v_g ($\text{km} \cdot \text{s}^{-1}$)	$\mathcal{F}_{\text{CMOR}}$ ($\text{hr}^{-1} \cdot \text{km}^{-2}$)
(139359) 2001 ME ₁	200	2006 Jun. 24	1924–1967	93°	191°	+4°	30.0	0.01
(247360) 2001 XU	100	2014 Dec. 14	1903–1993	263°	190°	+17°	29.1	0.02
(297274) 1996 SK	200	2007 Apr. 17	1870–1903	27°	2°	−3°	21.5	0.01
(435159) 2007 LQ ₁₉	200	2002 Jul. 13	1801–1978	111°	139°	+50°	14.1	0.01
..	..	2006 Jul. 13	1801–2003	111°	139°	+50°	14.1	0.03
..	..	2007 Jul. 13	1805–2003	111°	139°	+50°	14.1	0.04
2001 HA ₄	200	2005 Sep. 21	1807–1974	179°	184°	−20°	24.5	2.71
2005 WY ₅₅	1200	2002 May 31 [†]	994–1765	70°	8°	−12°	19.3	0.16
..	..	2006 May 31 [‡]	990–1753	70°	7°	−12°	19.5	0.14
..	..	2010 May 31	875–1761	70°	8°	−12°	19.4	0.06
..	..	2014 May 31	951–1725	70°	7°	−12°	19.5	0.05
2007 CA ₁₉	100	2012 Mar. 14	1965–1993	354°	185°	−10°	27.1	0.42
2009 SG ₁₈	200	2006 Sep. 20	1831–1852	178°	238°	+70°	34.1	0.01
..	..	2015 Sep. 21	1920–1931	178°	239°	+70°	34.3	0.01

Table 4—Continued

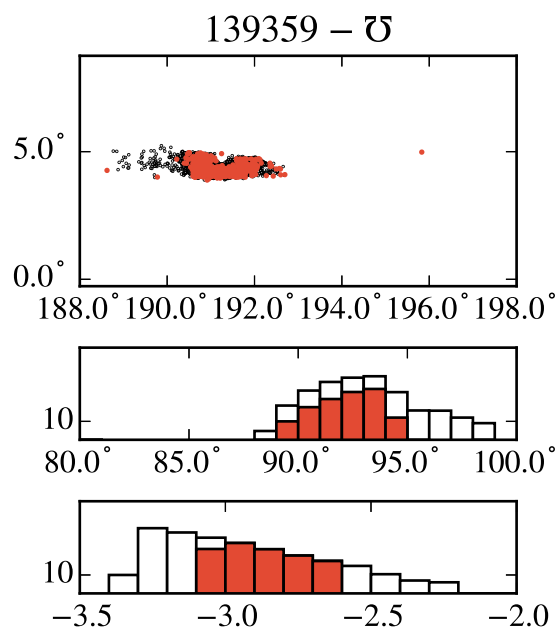
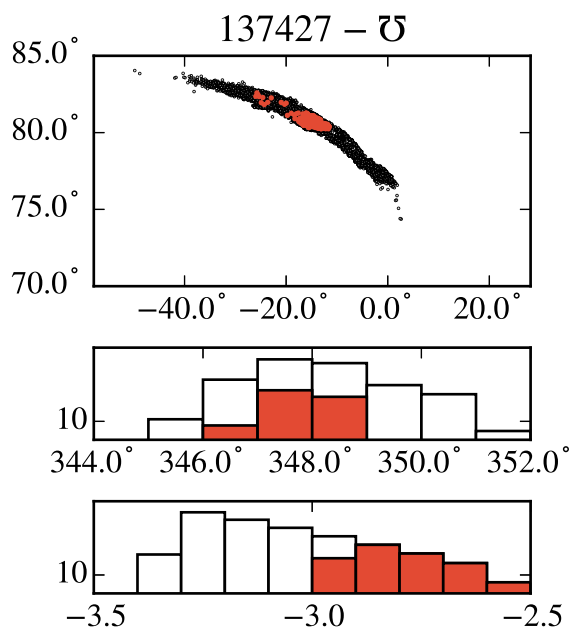
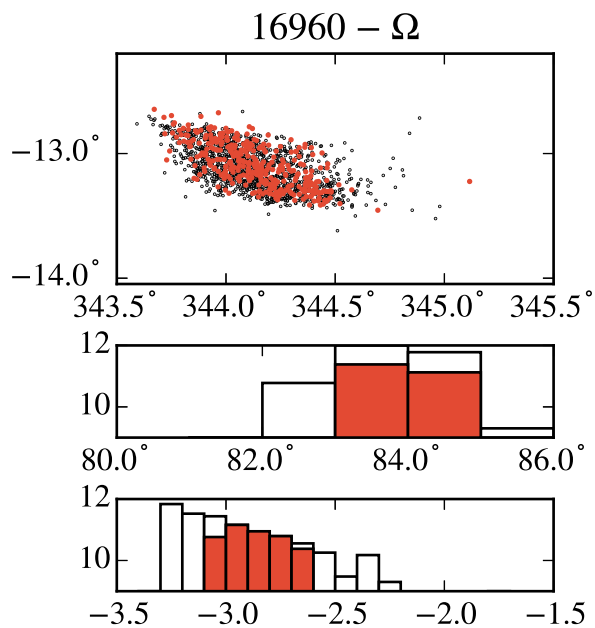
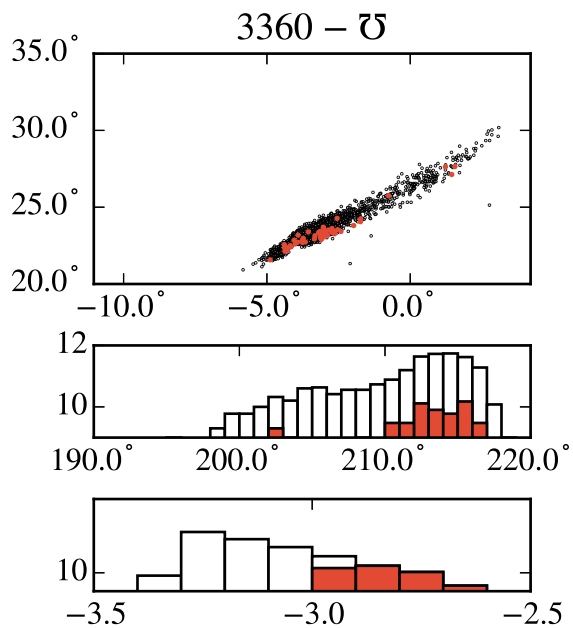
Parent	τ_{enc} (yr)	Date (UT)	Ejection	λ_{\odot}	$\lambda - \lambda_{\odot}$	β	v_g (km · s ⁻¹)	$\mathcal{F}_{\text{CMOR}}$ (hr ⁻¹ · km ⁻²)
2012 BU ₆₁	1100	2007 Jun. 29	1500–1788	97°	181°	−6°	23.9	0.05
2012 TO ₁₃₉	100	2012 Sep. 21	1954–2008	179°	345°	+4°	32.6	16.62
2015 TB ₁₄₅	100	2003 Oct. 31	1902–1997	218°	204°	−24°	34.9	12.62
..	..	2004 Oct. 31	1908–1979	218°	204°	−24°	35.0	0.01
..	..	2006 Oct. 31	1902–2000	218°	204°	−24°	34.9	23.54
..	..	2009 Oct. 31	1902–2006	218°	204°	−24°	34.9	42.86
..	..	2010 Oct. 31 [†]	1905–1991	218°	204°	−24°	34.9	0.14
..	..	2012 Oct. 31	1930–2009	218°	204°	−24°	34.8	10.95
..	..	2013 Oct. 31	1902–1982	218°	204°	−24°	34.9	0.10
..	..	2014 Oct. 31	1911–1960	218°	204°	−24°	35.0	0.01
..	..	2015 Oct. 31	1905–2015	218°	204°	−24°	34.9	9.42

[†]CMOR not operational during the day.

[‡]CMOR partially operational during the day.

Table 5. Orbits and radiant characteristics of the possible meteor activity associated to (139359) 2001 ME₁. Listed are perihelion distance q , eccentricity e , inclination i , longitude of ascending node Ω and argument of perihelion ω for the parent (taken from JPL 71) and the meteor outburst in 2006 (derived from the corresponding wavelet maximum). The uncertainties in the orbital elements for the parents are typically in the order of 10^{-5} to 10^{-8} in their respective units and are not shown. Epochs are in J2000.

	Orbital elements (J2000)					Geocentric radiant (J2000)			$\langle X \rangle$	
	q (AU)	e	i	Ω	ω	$\lambda - \lambda_{\odot}$	β	v_g (km s ⁻¹)	$H < 18$	$H < 22$ 53
(139359) 2001 ME ₁	0.35512	0.86598	5.796°	86.506°	300.254°	191° ±1°	+4° ±1°	30.0 ±0.1		
2006 outburst	0.32 ±0.02	0.87 ±0.03	4.7° ±1.4°	93.0° ±0.5°	298.8° ±2.2°	193.0° ±0.5°	+3.5° ±0.5°	30.5 ±0.5	0.01–0.02	0.1–0.3



This figure "fig-a1.png" is available in "png" format from:

<http://arxiv.org/ps/1607.07369v1>

This figure "fig-a2.png" is available in "png" format from:

<http://arxiv.org/ps/1607.07369v1>

This figure "fig-a3.png" is available in "png" format from:

<http://arxiv.org/ps/1607.07369v1>

This figure "fig-a4.png" is available in "png" format from:

<http://arxiv.org/ps/1607.07369v1>

This figure "fig-a5.png" is available in "png" format from:

<http://arxiv.org/ps/1607.07369v1>

This figure "fig-a6.png" is available in "png" format from:

<http://arxiv.org/ps/1607.07369v1>

This figure "fig-a7.png" is available in "png" format from:

<http://arxiv.org/ps/1607.07369v1>

This figure "fig-a8.png" is available in "png" format from:

<http://arxiv.org/ps/1607.07369v1>

This figure "fig-a9.png" is available in "png" format from:

<http://arxiv.org/ps/1607.07369v1>

This figure "fig-a10.png" is available in "png" format from:

<http://arxiv.org/ps/1607.07369v1>

This figure "fig-a11.png" is available in "png" format from:

<http://arxiv.org/ps/1607.07369v1>

This figure "fig-a12.png" is available in "png" format from:

<http://arxiv.org/ps/1607.07369v1>

This figure "fig-a13.png" is available in "png" format from:

<http://arxiv.org/ps/1607.07369v1>

This figure "fig-a14.png" is available in "png" format from:

<http://arxiv.org/ps/1607.07369v1>

